Journal of Molecular Liquids 319 (2020) 114359

Contents lists available at ScienceDirect

Journal of Molecular Liquids

journal homepage: www.elsevier.com/locate/molliq

Investigations of conformational structures and activities of trypsin and pepsin affected by food colourant allura red

Qi Xiao, Jiandan Liang, Huajian Luo, Haimei Li, Jing Yang, Shan Huang *

Guangxi Key Laboratory of Natural Polymer Chemistry and Physics, College of Chemistry and Materials, Nanning Normal University, Nanning 530001, PR China

ARTICLE INFO

Article history:
Received 21 July 2020
Received in revised form 19 August 2020
Accepted 16 September 2020
Available online 19 September 2020

Keywords:
Allura red
Trypsin
Pepsin
Binding interaction
Conformational structure
Enzymatic activity

ABSTRACT

Herein, binding interactions of food colourant allura red (AR) with trypsin and pepsin were comparably investigated for deep revelations of conformational structures and activities of proteinases affected by food colourant. Various results indicated that one AR bound with one proteinase to form novel ground state complex under the binding forces of van der Waal interactions and hydrogen bonds. Intrinsic fluorescence of proteinases was quenched by AR via static fluorescence quenching mode. Conformational structures of proteinases were all changed obviously after their binding interactions with AR, resulting in their structure transformation to the β-sheet structure. AR bound with the allosteric site of proteinases to inhibit their activities via non-competitive manner. Finally, AR protected human serum albumin from the digestion of proteinases efficiently. These results revealed the exact binding mechanisms of food colourant AR with proteinases, which illuminated the possible biological risk of food colourant AR on human beings.

1. Introduction

Allura red (AR), which is a kind of artificial azo dye, has been widely used in food and beverage industries [1,2]. Since AR can interact with target cells and cause malignant tumors, the excessive intake of AR into the human body can damage several living organisms and cause potential carcinogenic effects on human beings [3]. Consequently, on its first safety assessment, the acceptable daily intake of AR is 7 mg/kg body weight per day according to the Joint FAO/WHO Expert Committee on Food Additives [4]. Due to the vital multiple biological functions of serum proteins in blood plasma, the biological influences of AR on several serum proteins have been deeply investigated [5]. Several researches groups investigated the binding property between AR and human serum albumin (HSA) at the molecular level through several spectroscopic approaches and molecular modeling techniques [6–8]. Lelis and co-workers studied the interaction of AR with bovine serum albumin and further illustrated their binding thermodynamics [9]. All such investigations confirmed the binding interaction of AR with serum proteins and the structural variations of these proteins affected by AR. Consequently, the biological functions of serum proteins were changed by AR, supporting the hypothesis of the potential biological risk of AR to human health. However, the binding mechanism of AR on important biofunctional proteins is exceedingly complicated and remains largely unknown, although such revelations can be used to systematically evaluate the biological risks of AR on human beings. Undoubtedly, the biosafety evaluation of AR becomes the vital issue that must be clarified for their widespread application.

Proteinases play important roles in numerous catalyzing reactions during several physiological and pathological processes [10]. The investigations of conformational structures and activities of proteinases are very imperative to the exploration of effective and targeted drugs for proteinases-related diseases therapy. Trypsin (EC 3.4.21.4) is a type of serine proteinase [11,12] while pepsin (EC 3.4.23.1) is a representative aspartic proteinase [13,14]. Trypsin and pepsin are proved to play important biological roles in the digestion and decomposition of several physiological processes in human digestive system. Consequently, both of them are often chosen as binding model proteinases to illuminate the biological influences of small molecules those founded in food on their conformational structures and activities. Freitas et al. studied the interaction between grape seed procyanidins and trypsin, and their results proved that procyanidins affected the conformational structure of trypsin slightly [15]. Wang et al. investigated the interactions between five chlorophenols and trypsin, and their results showed that the number of chlorine atoms of chlorophenols partly affected the binding ability of them with trypsin [16]. The binding interactions of sunset yellow, curcumin, and Ligupurpuroside A with pepsin have also been revealed [13,14,17]. The influences of phenylpropanoid glycosides and folic acid on the conformations and activities of trypsin and pepsin were studied by Wu's group and Fei's group [18,19]. However, the variations of conformational structures and activities of trypsin and pepsin after their interactions with food colourant AR have not been reported

* Corresponding author.
E-mail address: huangs@whu.edu.cn (S. Huang).

https://doi.org/10.1016/j.molliq.2020.114359
0167-7322/

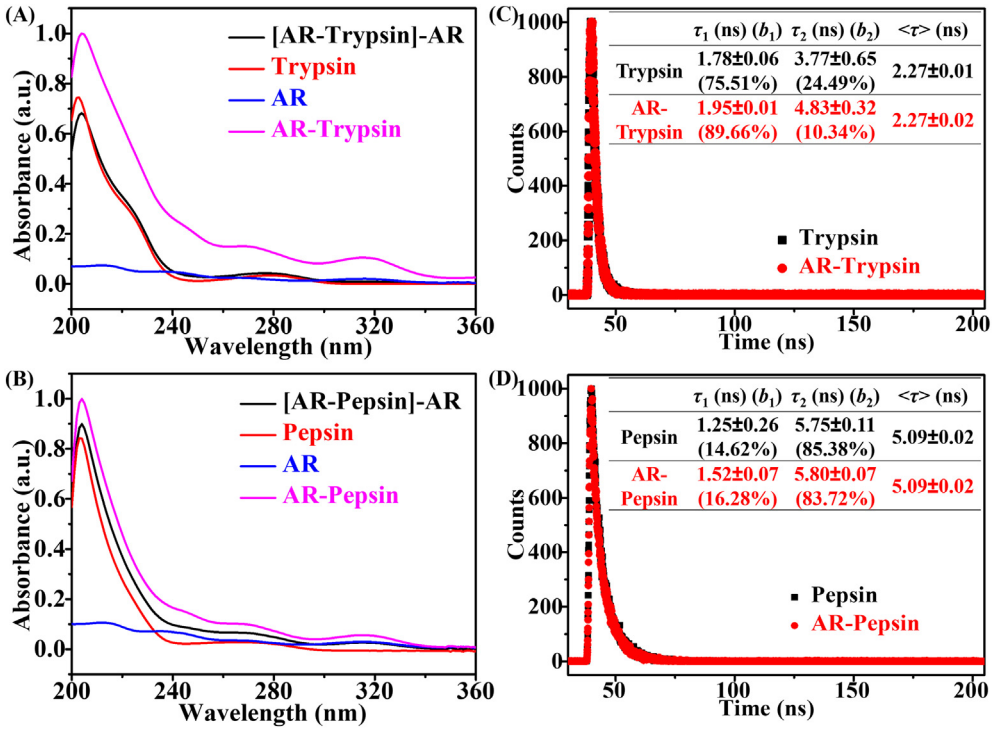

	τ_1 (ns) (b_1)	τ_2 (ns) (b_2)	<τ> (ns)
Trypsin	1.78±0.06 (75.51%)	3.77±0.65 (24.49%)	2.27±0.01
AR-Trypsin	1.95±0.01 (89.66%)	4.83±0.32 (10.34%)	2.27±0.02

	τ_1 (ns) (b_1)	τ_2 (ns) (b_2)	<τ> (ns)
Pepsin	1.25±0.26 (14.62%)	5.75±0.11 (85.38%)	5.09±0.02
AR-Pepsin	1.52±0.07 (16.28%)	5.80±0.07 (83.72%)	5.09±0.02

Fig. 1. (A) UV–vis absorption spectra of trypsin, AR, AR-trypsin system, and the difference absorption spectrum between AR-trypsin system and AR. (B) UV–vis absorption spectra of pepsin, AR, AR-pepsin system, and the difference absorption spectrum between AR-pepsin system and AR. The concentrations of proteinases and AR were all 4.0×10^{-6} mol L^{-1}. (C) Fluorescence decay traces of trypsin before and after the addition of AR. (D) Fluorescence decay traces of pepsin before and after the addition of AR. The concentrations of proteinases and AR were all 4.0×10^{-6} mol L^{-1}. τ is the fluorescent lifetime of proteinase and b is the normalized pre-exponential factor, respectively.

as far as we know. Such investigations can be used to evaluate the biological risk of AR on human beings more deeply and objectively.

Herein, the binding interactions of AR with trypsin and pepsin were investigated by using several experimental approaches and molecular modeling technique. Detailed binding mechanisms between proteinases and AR will be elucidated through this research. Such researches can further explore the variations of conformational structures and activities of proteinases after their binding interactions with AR. Through such investigation, we expect to provide valuable and meaningful information to the biological effect evaluation of food colourant AR in health-related fields.

2. Material and methods

2.1. Materials

Trypsin (from bovine pancreas), pepsin (from porcine gastric mucosa), HSA, AR, hemoglobin (from bovine erythrocyte), *N*-alpha-Benzoyl-DL-arginine-4-nitroanilide hydrochloride (BApNA, ≥98%), and *p*-nitroaniline (pNA) were all purchased from Sigma-Aldrich Co., Ltd. (St. Lousi, USA). Trypsin was dissolved in 20 mM of phosphate buffer saline (PBS, pH 7.4). Pepsin was dissolved in 20 mM of citric acid solution (pH 2.0). All other chemical reagents were of analytical reagent grade and used as received without any additional processes. Ultrapure water with a resistivity of 18.2 MΩ cm was produced by Millipore-Q Academic purification set (Millipore, Bedford, MA, USA) and used in the whole experiments.

2.2. UV–vis absorption spectroscopy

UV–vis absorption spectra of proteinases, AR, and AR-proteinase systems were recorded on Cary 100 UV–vis spectrophotometer (Agilent Technologies, Inc., Australia). The difference absorption spectra between AR-proteinase systems and AR were measured by using AR as the reference. The measuring wavelength was decreased from 360 to 200 nm with 1 nm interval and the scan speed was 600 nm min^{-1}. Quartz cells with 1.0 cm path-length were used for all measurements. The concentrations of proteinases and AR were all 4.0×10^{-6} mol L^{-1}.

Proteinase activity experiments were proceeded by using BApNA and hemoglobin as substrates for trypsin and pepsin according to the reported literature [20,21]. For evaluation of trypsin activity, 5.0 mL of BApNA with different concentration, 0.2 mL of trypsin (0.25 g L^{-1}), and 4.8 mL of Tris-HCl buffer (pH 8.2) were mixed completely and incubated at 37 °C for 10 min. The absorbance of the solution at 400 nm was measured to evaluate the trypsin activity. For evaluation of pepsin activity, 2.0 mL of hemoglobin with different concentration, 1.0 mL of pepsin (1.0 g L^{-1}), and 2.0 mL of citric acid buffer (pH 2.0) were mixed completely and incubated at 37 °C for 30 min. Then, 2.0 mL of trichloroacetic acid (10%) was added to stop the enzymatic reaction. The mixture was centrifuged at 12,000 rpm for 10 min, and the supernatant was transferred into another new test tube. Finally, the absorbance of the solution at 275 nm was measured to evaluate the pepsin activity. The scan speed was 600 nm min^{-1} and quartz cells (1.0 cm path-length) were used for all measurements. The concentration of trypsin and pepsin were 2.1×10^{-7} and 5.6×10^{-6} mol L^{-1}, respectively. The concentration of BApNA was increased from 5.7×10^{-5} to 9.2×10^{-4} mol L^{-1}. The concentration of hemoglobin was increased from 7.8×10^{-6} to 7.8×10^{-5} mol L^{-1}. The concentration of AR was increased from 0 to 3.6×10^{-4} mol L^{-1} with interval of 1.2×10^{-4} mol L^{-1}.

2.3. Fluorescence spectroscopy

Time-resolved fluorescence spectra of proteinases and AR-proteinase systems were recorded on Horiba Scientific QM-8075 high sensitivity steady-state transient fluorescence spectrometer (HORIBA, Japan) with time-correlated single-photo counting system.

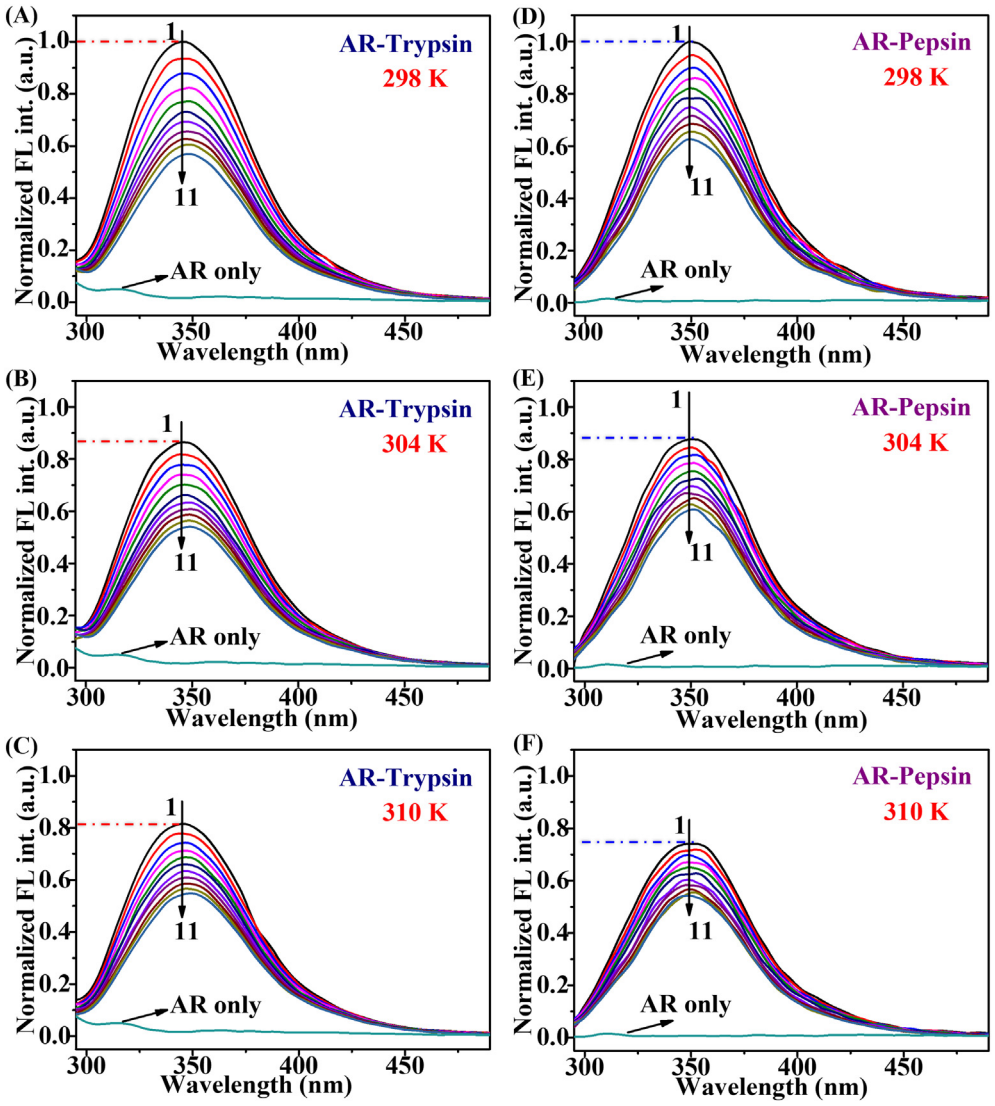

Fig. 2. Steady-state fluorescence spectra of trypsin with increasing concentration of AR at 298 (A), 304 (B), and 310 K (C). Steady-state fluorescence spectra of pepsin with increasing concentration of AR at 298 (D), 304 (E), and 310 K (F). The concentrations of proteinases were all 4.0×10^{-6} mol L^{-1}. The concentrations of AR were (1–11, $\times 10^{-6}$ mol L^{-1}): 0, 1, 2, 3, 4, 5, 6, 7, 8, 9, and 10, respectively.

Fluorescence decay traces were recorded at room temperature with excitation/emission wavelengths of 278/350 nm/nm, respectively. The slits of the excitation and the emission were all 8.0 nm. Fluorescence decay traces were fitted with the biexponential function. The average fluorescent lifetime ($<\tau>$) was calculated by the equation of $<\tau> = \Sigma \tau_i b_i$ (τ is the fluorescent lifetime of proteinase and b is the normalized pre-exponential factor) [22]. Each data was the average of three times successive scanning. The concentrations of proteinases and AR were all 4.0×10^{-6} mol L^{-1}.

Steady-state fluorescence spectra of proteinases with different concentrations of AR at 298, 304, and 310 K were performed on Perkin-Elmer LS 55 luminescence spectrometer (Waltham, MA, USA) with a thermostatic bath. Fluorescence spectra were recorded with excitation/emission wavelengths of 280/350 nm/nm, respectively. The slits of the excitation and the emission for AR-trypsin system were 15 and 18 nm, respectively. The slits of the excitation and the emission for AR-pepsin system were 9 and 6.5 nm, respectively. The scan speed was 600 nm min^{-1}. Each spectrum was the average of three times successive scanning. The concentrations of proteinases were all 4.0×10^{-6} mol L^{-1}, and the concentration of AR was increased from 0 to 1.0×10^{-5} mol L^{-1} with interval of 1.0×10^{-6} mol L^{-1}. When researching the influences of co-existed metal ions on AR-proteinase systems, the steady-state fluorescence spectra of AR-proteinase systems were recorded at 298 K after the addition of metal ions (4.0×10^{-6} mol L^{-1}). Other experimental parameters were all remained as previously mentioned.

Three-dimensional fluorescence spectra of proteinases and AR-proteinase systems were performed on Perkin-Elmer LS 55 luminescence spectrometer (Waltham, MA, USA). The excitation wavelength was increased from 200 to 350 nm and the emission wavelength was changed from 200 to 500 nm with 5 nm increment. The slits of the excitation and the emission for trypsin and AR-trypsin system were 15 and 18 nm, respectively. The slits of the excitation and the emission for pepsin and AR-pepsin system were 9 and 6.5 nm, respectively. The scan speed was 600 nm min^{-1}. The concentrations of proteinases and AR were all 2.0×10^{-6} mol L^{-1}.

2.4. Fourier transform infrared spectroscopy

Fourier transform infrared (FT-IR) spectra of proteinases and AR-proteinase systems were recorded on Perkin-Elmer Frontier spectrometer (Waltham, MA, USA) via the zinc selenide attenuated total

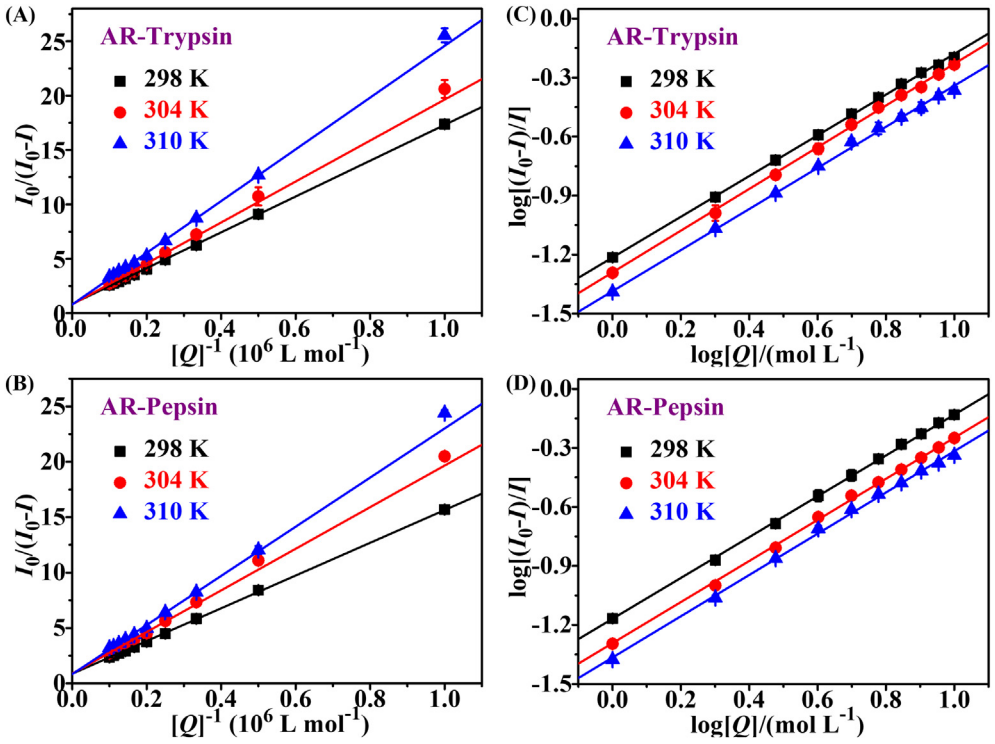

Fig. 3. Modified Stern-Volmer plots of AR-trypsin system (A) and AR-pepsin system (B) at three different temperatures. Double-logarithmic plots of AR-trypsin system (C) and AR-pepsin system (D) at three different temperatures.

reflection method with 128 interferograms and resolution of 4 cm^{-1}. The difference FT-IR spectra between AR-proteinase systems and AR were measured by using AR as the reference. The subtraction of the reference spectrum from the spectrum of the buffer solution was carried out in accord with the criteria that straight baseline was obtained between 2000 and 1750 cm^{-1} [23]. The percentages of different secondary structures of proteinases were estimated by Omnic data processing software combined with Fourier deconvolution and curve fitting from 1700 to 1600 cm^{-1} [24]. The peak positions and the half widths of each sub-peak were estimated with the peak width of 48.8 and the enhancement of 3.2. After determining the correspondences between each sub-peak and different secondary structures, the relative percentages of various secondary structures were calculated according to their integrated areas. The concentrations of proteinases and AR were all 1.0×10^{-3} mol L^{-1}.

2.5. Circular dichroism spectroscopy

Circular dichroism (CD) spectra of proteinases, AR, and AR-proteinase systems were recorded on Chirascan CD spectrometer (Applied Photophysics, England) at 25 °C under the constant nitrogen flush protection. When recording the CD spectra of AR-proteinase systems with different molar ratio of AR to proteinase under different reaction temperatures, the temperature was increased from 20 to 90 °C in 5 °C steps with 300 s increments. The melting temperature (T_m) and the molar enthalpy change (ΔH_m) at that temperature were measured by CD spectrometer equipped with the Global Analysis Software. The percentages of different secondary structures of proteinases were analyzed via the CD neural networks (CDNN) software [25]. The scan speed was 500 nm min^{-1} and the response time was 0.5 s. Each spectrum was the average of three times successive scanning. The concentrations of trypsin and pepsin were 2.5×10^{-5} and 2.5×10^{-6} mol L^{-1}. The concentrations of AR were one or two times of the proteinase concentrations.

2.6. Electrochemical investigation

Electrochemical experiments were all performed on Chenhua CHI-660E electrochemical workstation (Shanghai, China) with conventional three-electrode electrochemical testing system. The electrolyte is 5.0 mM of $K_3Fe(CN)_6/K_4Fe(CN)_6$ solution with 10 mM of KCl. Gold electrode (GE), Ag/AgCl electrode, and platinum wire were served as working electrode, reference electrode, and counter electrode, respectively. For the preparation of proteinases modified GE (Trypsin/GE and

Table 1
Binding constants K_a, binding constants K_b, binding number n, and relative thermodynamic parameters in AR-proteinase systems.

System	T (K)	K_a (10^4 L mol^{-1})	R^{2a}	K_b (10^4 L mol^{-1})	n	R^{2a}	ΔH (kJ mol^{-1})	ΔG (kJ mol^{-1})	ΔS (J mol^{-1} K^{-1})	R^{2a}
	298	5.12 ± 0.54	0.999	6.11 ± 0.08	1.03	0.999		−26.75 ± 0.007		
AR-trypsin	304	4.27 ± 0.25	0.999	5.13 ± 0.34	1.06	0.999	−48.73 ± 0.16	−26.31 ± 0.001	−73.78 ± 0.52	0.999
	310	3.32 ± 0.35	0.999	4.12 ± 0.41	1.04	0.999		−25.86 ± 0.007		
	298	5.91 ± 0.49	0.999	6.79 ± 0.25	1.04	0.999		−27.30 ± 0.17		
AR-pepsin	304	4.72 ± 0.17	0.999	5.10 ± 0.12	1.04	0.998	−65.72 ± 0.98	−26.52 ± 0.20	−128.93 ± 3.86	0.999
	310	3.77 ± 0.21	0.999	4.31 ± 0.07	1.04	0.999		−25.75 ± 0.22		

[a] R^2 is the correlation coefficient.

Table 2
Binding constants K_a of AR-proteinase systems in the absence and presence of different common metal ions.

System	K_a (10^4 L mol^{-1})	R^{2a}	S.D.[b]	K/K_a
AR-trypsin alone	5.12 ± 0.54	0.999	0.01	1
AR-trypsin-Mg^{2+}	4.78 ± 0.05	0.999	0.04	0.93
AR-trypsin-Ca^{2+}	4.86 ± 0.19	0.999	0.09	0.95
AR-trypsin-Cu^{2+}	4.61 ± 0.23	0.999	0.17	0.90
AR-trypsin-Al^{3+}	4.79 ± 0.13	0.999	0.19	0.94
AR-trypsin-Zn^{2+}	4.72 ± 0.05	0.999	0.13	0.92
AR-trypsin-Cr^{3+}	4.71 ± 0.31	0.999	0.18	0.92
AR-trypsin-Pb^{2+}	4.67 ± 0.08	0.999	0.11	0.91
AR-trypsin-Mn^{2+}	4.82 ± 0.18	0.998	0.07	0.93
AR-trypsin-Fe^{2+}	4.88 ± 0.14	0.999	0.13	0.95
AR-trypsin-Fe^{3+}	4.89 ± 0.25	0.999	0.16	0.96
AR-pepsin alone	5.91 ± 0.49	0.999	0.01	1
AR-pepsin-Mg^{2+}	5.29 ± 0.20	0.999	0.20	0.90
AR-pepsin-Ca^{2+}	5.14 ± 0.17	0.999	0.17	0.87
AR-pepsin-Cu^{2+}	5.29 ± 0.05	0.999	0.05	0.90
AR-pepsin-Al^{3+}	5.15 ± 0.13	0.999	0.13	0.87
AR-pepsin-Zn^{2+}	5.25 ± 0.27	0.999	0.06	0.89
AR-pepsin-Cr^{3+}	4.92 ± 0.13	0.999	0.13	0.83
AR-pepsin-Pb^{2+}	5.21 ± 0.18	0.999	0.18	0.88
AR-pepsin-Mn^{2+}	5.12 ± 0.12	0.999	0.12	0.87
AR-pepsin-Fe^{2+}	5.17 ± 0.08	0.999	0.12	0.87
AR-pepsin-Fe^{3+}	5.23 ± 0.12	0.999	0.08	0.89

[a] R^2 is the correlation coefficient.
[b] *S.D.* is standard deviation.

Pepsin/GE), 10 μL of proteinases solution (5.0×10^{-6} mol L^{-1}) were dropped onto the surface of bare GE. The electrode was then incubated at 4 °C for 1 h. The proteinases modified GE were washed by ultrapure water for three times and then were dried in nitrogen airflow. For cyclic voltammograms (CV) and electrochemical impedance spectrum (EIS) measurements, different concentration of AR was added into the electrolyte solution and then stirred for 5 min. The reaction system was at rest for 3 min before testing. CV was recorded with scan rate of 50 mV s^{-1} and EIS was measured within the frequency range from 0.1 to 100 kHz. Each spectrum was the average of three times successive scanning. The concentration of AR was increased from 6.0×10^{-6} to 6.0×10^{-5} mol L^{-1} with interval of 6.0×10^{-6} mol L^{-1}.

2.7. Molecular modeling

Crystal structures of trypsin (PDB ID: 2ZQ1) and pepsin (PDB ID: 3PEP) were taken from the RCSB Protein Data Bank [26,27]. The binding interactions of proteinases with AR were researched by using Surflex Dock program in Sybyl-X 2.0 software with energy termination gradient of 0.01 kcal mol^{-1} [28]. The molecular structure was optimized by the Tripos force field. The AR molecule was charged by the Gasteiger and Hückel methods. The protomol for trypsin and pepsin were all generated by the ligand mode. The threshold was 0.50 and the bloat was 3.0. The parameters in the docking work were same with the previously reported data [28].

2.8. Sodium dodecyl sulfate-polyacrylamide gel electrophoresis

Sodium dodecyl sulfate-polyacrylamide gel electrophoresis (SDS-PAGE) of substrate HSA with proteinases at the present of different concentration of AR was performed using vertical electrophoresis system (Bio-Rad, U.K.) [29]. The concentrations of HSA, trypsin, and pepsin were 6.0×10^{-6}, 2.5×10^{-5}, and 1.1×10^{-5} mol L^{-1}, respectively. The concentration of AR was increased from 0 to 2.4×10^{-2} mol L^{-1} with interval of 8.0×10^{-3} mol L^{-1}. AR with different concentration and proteinase were firstly mixed completely and incubated at 37 °C water bath for 30 min. Then, HSA was added into the solution and the mixture was continuously heated at 37 °C water bath for 10 min. Phenylmethanesulfonyl fluoride was added to terminate the enzymatic reaction. The treated sample was mixed with four times of the loading buffer (0.5 mol L^{-1} of Tris-HCl, pH 6.8, 5% (w/v) SDS, 20% (v/v) glycerol). The mixture was boiled for 5 min and then was cooled to room

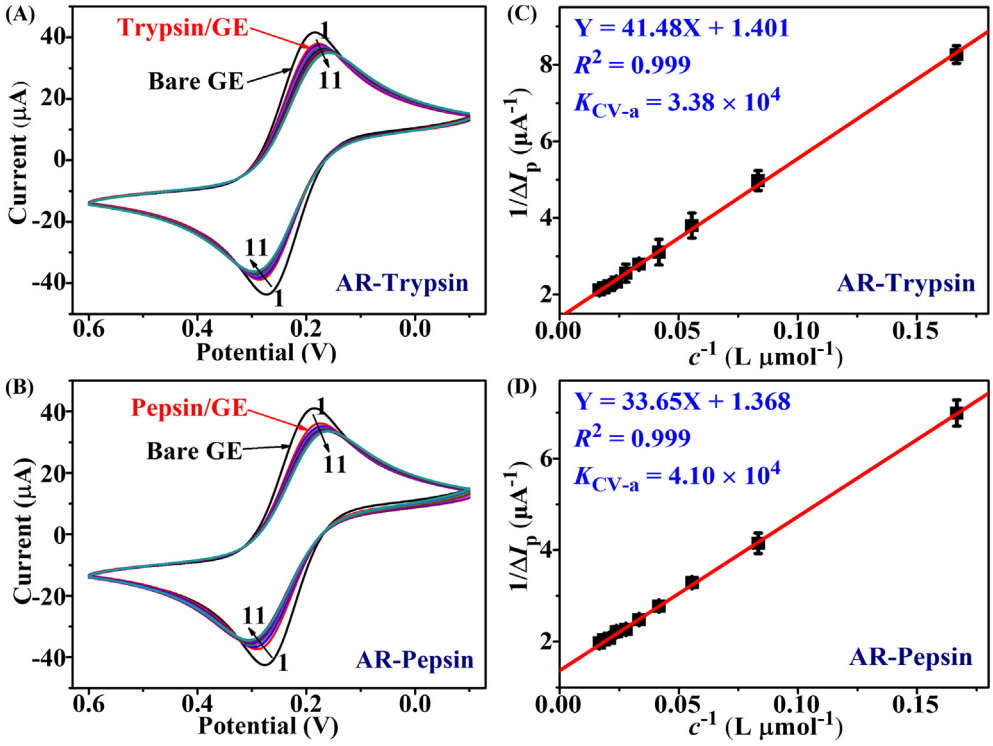

Fig. 4. (A) CV of GE and Trypsin/GE with different concentration of AR. (B) CV of GE and Pepsin/GE with different concentration of AR. Linear relationships between $1/\Delta I_p$ and $1/c$ in AR-trypsin system (C) and AR-pepsin system (D). The concentrations of AR were (1–11, $\times 10^{-6}$ mol L^{-1}): 0, 6, 12, 18, 24, 30, 36, 42, 48, 54, and 60, respectively.

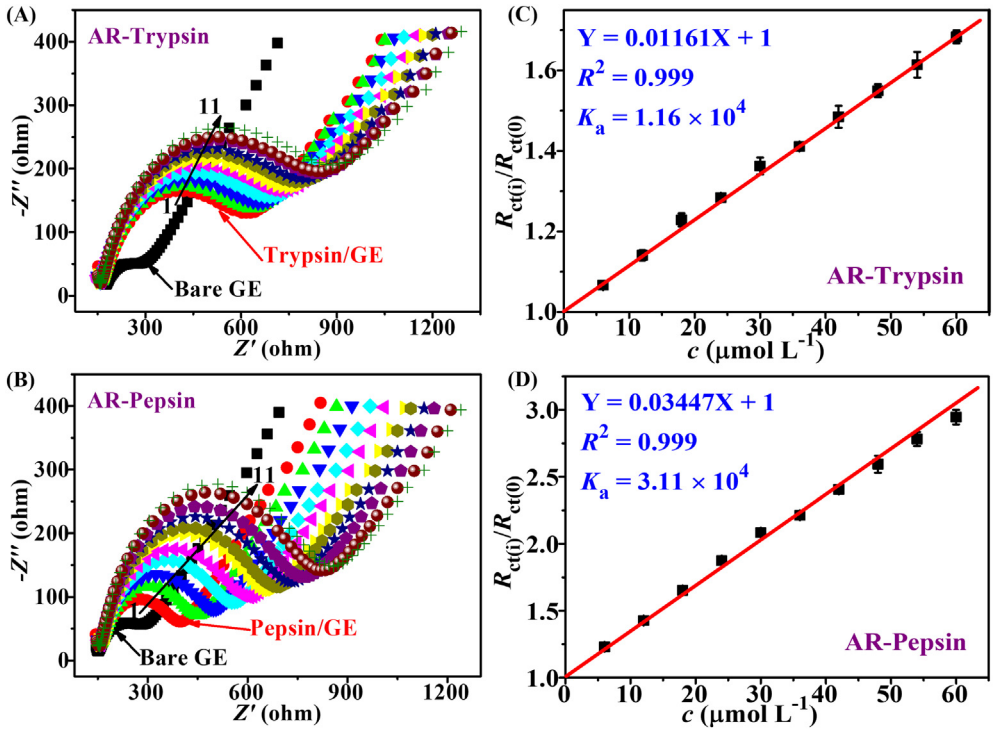

Fig. 5. (A) EIS of GE and Trypsin/GE with different concentration of AR. (B) EIS of GE and Pepsin/GE with different concentration of AR. Linear relationships between $R_{ct(i)}/R_{ct(0)}$ and c in AR-trypsin system (C) and AR-pepsin system (D). The concentrations of AR were (1–11, $\times 10^{-6}$ mol L^{-1}): 0, 6, 12, 18, 24, 30, 36, 42, 48, 54, and 60, respectively.

temperature gradually. The experiments were performed in 5% (w/v) stacking gel and 14% (w/v) separating gel. The low molecular weight marker from 14.3 to 97.2 KDa was used to estimate the molecular weight of the sample. After electrophoresis, the gel was stained with Coomassie brilliant blue R-250 in staining solution (30% (v/v) methanol, 10% (v/v) acetic acid, and 60% (v/v) water) for 30 min. The gel was de-stained in de-staining solution (30% (v/v) methanol, 10% (v/v) acetic acid, and 60% (v/v) water) for additional 30 min. Finally, the clear protein bands on the gel indicated the presence of protease activity.

3. Results and discussion

3.1. Binding interactions between proteinases and AR

3.1.1. Binding mechanisms

Binding mechanisms between proteinases and AR are firstly verified by using UV–vis absorption spectroscopy. As exhibited in Fig. 1A and B, trypsin and pepsin showed a strong absorption peak at 204 nm and a typical absorption peak at 280 nm. These peaks are ascribed to peptide structures and the amino acid residues [tryptophan (Trp), tyrosine (Tyr), and phenylalanine (Phe)] in the structure of proteinases [22,30]. AR showed almost no obvious absorption from 200 to 360 nm. Meanwhile, the difference absorption spectrum between AR-trypsin system and AR did not cover perfectly with the UV–vis absorption spectrum of trypsin. Same situation was existed in pepsin and AR-pepsin system. It has been reported that if the absorption spectrum of fluorophore changes after the addition of compound, this compound should bind with fluorophore to form novel ground state complex [31]. Consequently, AR may bind with trypsin and pepsin to construct ground state complexes.

Such speculation can be further proved by time-resolved fluorescence spectroscopy. Fluorescence decay traces of proteinases without or with AR were illustrated in Fig. 1C and D. The fluorescent lifetime (τ) of proteinases consists of two parts: a short lifetime τ_1 and a long lifetime τ_2. The average fluorescent lifetime ($<\tau>$) is fitted with the equation of $<\tau> = \Sigma \tau_i b_i$ (b is the normalized pre-exponential factor) [22]. As shown in Fig. 1C and D, the average fluorescent lifetimes of trypsin and pepsin were calculated to be around (2.27 ± 0.01) and (5.09 ± 0.02) ns, respectively. The addition of AR did not change the average fluorescent lifetimes of proteinases at all. The fluorescent lifetime of fluorophore remains to its initial value if compound binds with fluorophore to form ground state complex [31]. Thus, AR should bind with trypsin and pepsin to form ground state complexes, which agrees perfectly with the previous results.

3.1.2. Binding constants and binding numbers

Binding constants among AR-proteinase systems can be obtained via recording the fluorescence spectra of proteinase with increasing concentration of AR under 298, 304, and 310 K. As shown in Fig. 2, two proteinases exhibited characteristic and intrinsic fluorescence peak at 350 nm under the excitation of 278 nm, but AR showed no absorption ability during the same wavelength range. In addition, the influence of temperature on the fluorescence intensity of pepsin was much higher than that of trypsin (red and blue dotted lines in Fig. 2). The intrinsic fluorescence of proteinases was all quenched by AR through concentration-dependent manner. Comparably, 1.0×10^{-5} mol L^{-1} of AR quenched the intrinsic fluorescence of trypsin to be about 43.1% at 298 K, while 1.0×10^{-5} mol L^{-1} of AR quenched the intrinsic fluorescence of pepsin to be about 37.4% at 298 K, confirming the stronger fluorescence quenching ability of AR on trypsin. Due to the ground state complexes formation between AR and proteinases, AR can quench the intrinsic fluorescence of proteinases through static quenching mode. Undoubtedly, binding constant (K_a) among AR-proteinase systems can be calculated via modified Stern-Volmer equation [32]:

$$\frac{I_0}{I_0 - I} = \frac{1}{f_a K_a}\frac{1}{[Q]} + \frac{1}{f_a} \quad (1)$$

In Eq. (1), I_0 and I are the fluorescence intensities of proteinases without and with AR, [Q] is the concentration of AR, and f_a is the mole

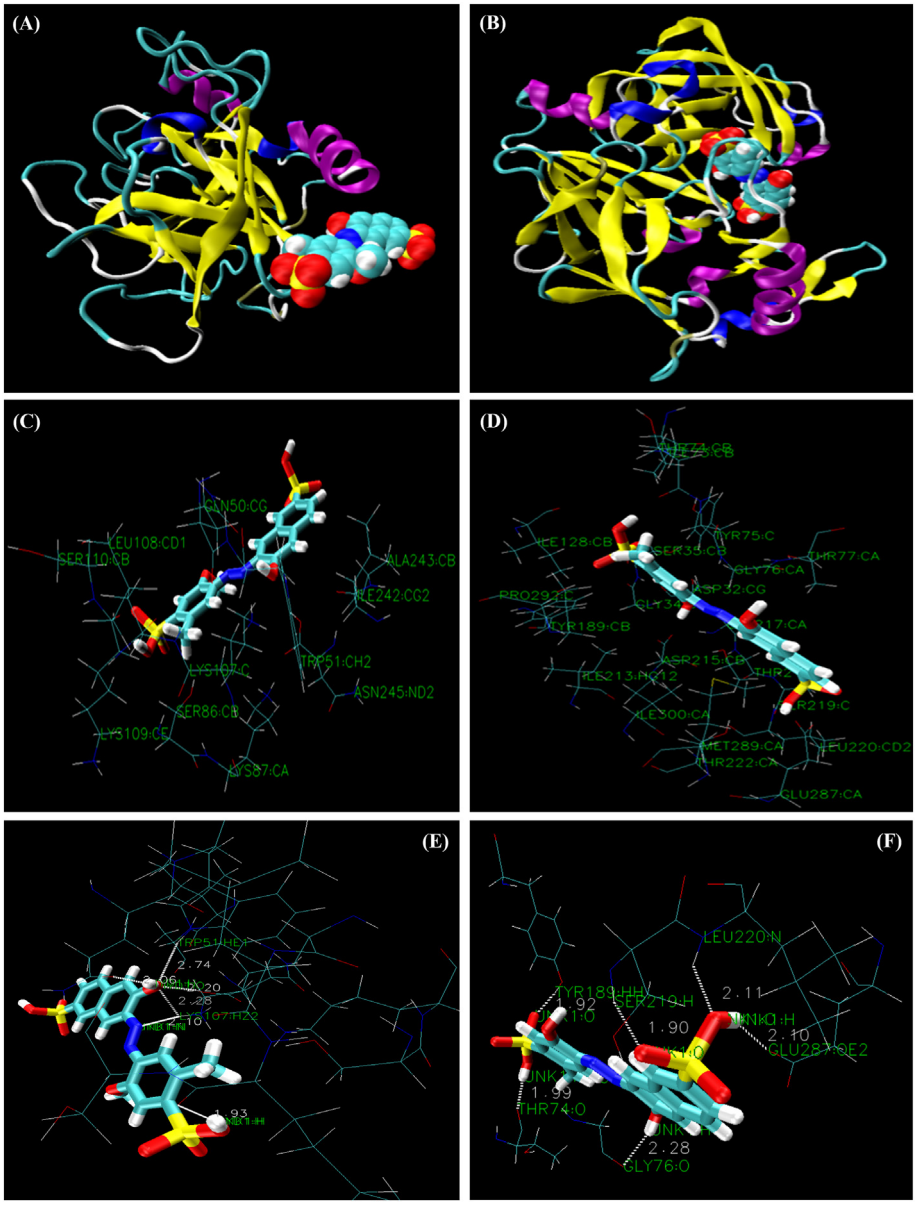

Fig. 6. Lowest binding energy conformation of the surface binding mode of AR with trypsin (A) and pepsin (B). Surrounded amino acid residues of trypsin (C) and pepsin (D) in AR molecule. Hydrogen bonds between amino acid residues of trypsin (E) and pepsin (F) and AR molecule.

fraction of solvent-accessible fluorophore, respectively [32]. Modified Stern-Volmer plots of AR-proteinase systems at three different temperatures were shown in Fig. 3A and B. The K_a values of AR-proteinase systems at three different temperatures were calculated and listed in Table 1. Since the K_a values of AR-proteinase systems were decreased gradually with the increase of temperature, reconfirming the static fluorescence quenching mechanism of AR-proteinase systems [23]. The K_a values of AR-proteinase systems were decreased to some extent when common metal ions were present (Table 2), indicating that common metal ions affected the binding interactions of AR with trypsin and pepsin obviously.

Binding constant (K_b) is further calculated by the traditional double-logarithmic equation [33]:

$$\log\frac{I_0-I}{I} = \log K_b + n\log[Q] \quad (2)$$

The binding number (n) can be also obtained through Eq. (2) if the compound binds with fluorophore at the same site [33]. Finally, the double-logarithmic plots of AR-proteinase systems were shown in Fig. 3C and D, and both the K_b values and the n values were all illustrated in Table 1. The K_b values were all decreased gradually with the increment of temperature, but the n values were almost constant to be one. Therefore, AR strongly bound with one proteinase to form ground state complexes.

On the other hand, binding constant can be also calculated through electrochemical methods, including CV and EIS [23,33]. As indicated in Fig. 4A and B, after the successful assembling of proteinases on the surface of GE, the redox peak currents of $K_3Fe(CN)_6/K_4Fe(CN)_6$ were decreased significantly due to the enhanced steric hindrance effect. The redox peak currents of $K_3Fe(CN)_6/K_4Fe(CN)_6$ were decreased step by step after the addition of increasing concentrations of AR, informing the improved electrostatic repulsion of $K_3Fe(CN)_6/K_4Fe(CN)_6$ toward the modified electrodes [23]. All these phenomena confirmed the binding interactions between AR and proteinases. The binding constant obtained by CV ($K_{CV\text{-}a}$) can be calculated through the plot of the reciprocal of the current drop (ΔI_p) and the reciprocal of AR concentration (c) according to the Langmuir equation [23]:

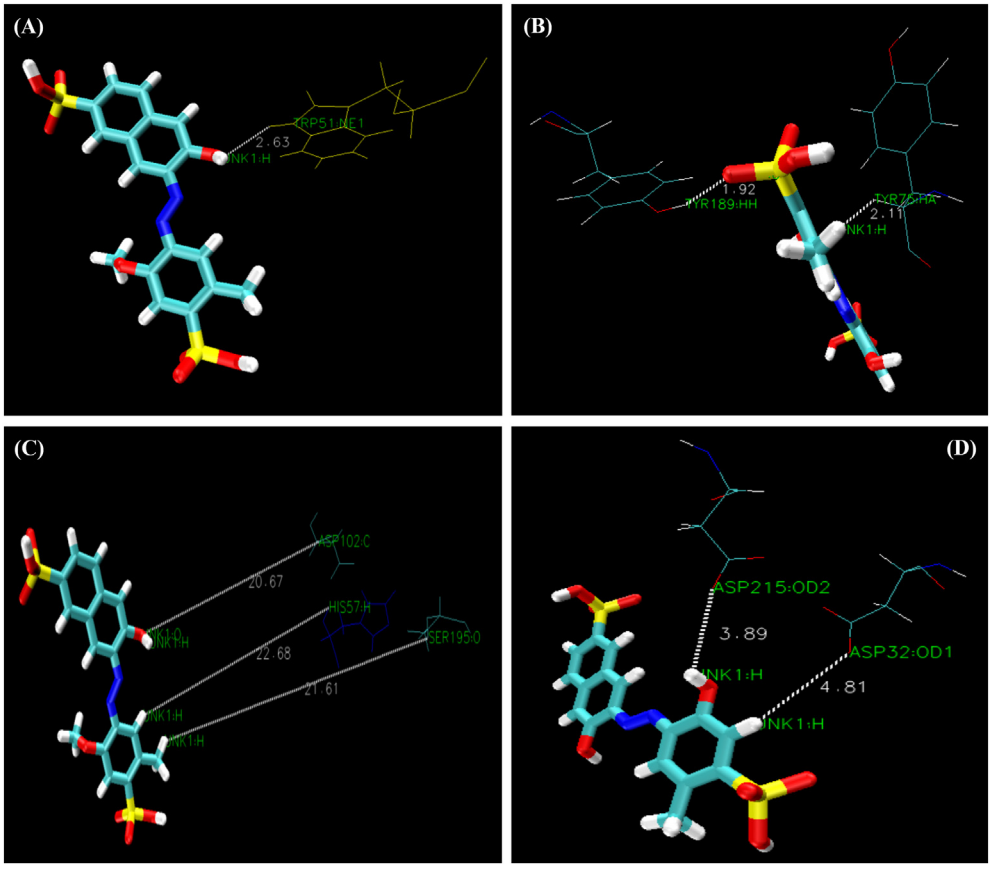

Fig. 7. Distances between AR molecule and the nearest fluorescent amino acids of trypsin (A) and pepsin (B). Distances between AR molecule and the catalytic amino acids of trypsin (C) and pepsin (D).

$$\frac{1}{\Delta I_p} = \frac{1}{\Delta I_{p,\,max}} + \frac{1}{\Delta I_{p,\,max} K_{CV-a} c} \tag{3}$$

The plots between $1/\Delta I_p$ and $1/c$ of AR-proteinase systems were shown in Fig. 4C and D. The linear fitting equations of AR-proteinase systems were $1/\Delta I_p$ [μA^{-1}] = 1.401 + 41.48/c [L μmol^{-1}] for AR-trypsin and $1/\Delta I_p$ [μA^{-1}] = 1.368 + 33.65/c [L μmol^{-1}] for AR-pepsin with correlation coefficient of 0.999. The $K_{CV\text{-}a}$ values were calculated to be 3.38×10^4 L mol^{-1} in AR-trypsin system and 4.10×10^4 L mol^{-1} in AR-pepsin system, respectively.

As further shown in Fig. 5A and B, the semicircle diameter at higher frequency of EIS curve was increased dramatically after surficial assembling of proteinases on GE. This semicircle diameter often indicates the charge-transfer resistance (R_{ct}) of the electrode [34], so the R_{ct} value was increased after the modification of proteinases on GE surface. The R_{ct} value was continuously increased with the increasing concentration of AR, ascribing to the enhanced charge-transfer resistance of the modified electrodes after the binding interactions of AR with proteinases. The binding constant obtained by EIS ($K_{EIS\text{-}a}$) can be calculated through the plot of the R_{ct} value and the AR concentration (c) according to the following equation [34]:

$$\frac{R_{ct(i)}}{R_{ct(0)}} = K_{ESI-a} c + 1 \tag{4}$$

The plots between $R_{ct(i)}/R_{ct(0)}$ and c were shown in Fig. 5C and D. The linear fitting equation of AR-trypsin was $R_{ct(i)}/R_{ct(0)}$ = 0.01161c [$\mu mol\ L^{-1}$] + 1 with correlation coefficient of 0.999 (Fig. 5C), while the linear fitting equation of AR-pepsin was $R_{ct(i)}/R_{ct(0)}$ = 0.03447c [$\mu mol\ L^{-1}$] + 1 with correlation coefficient of 0.999 (Fig. 5D). The $K_{EIS\text{-}a}$ values were 1.16×10^4 L mol^{-1} in AR-trypsin system and 3.11×10^4 L mol^{-1} in AR-pepsin system, respectively. Due to the natural conformation variation of proteinases and the enhanced steric hindrance effect, the binding interaction between proteinases and AR can be inhibited. Consequently, the binding constants calculated by electrochemical approaches are a little lower than those obtained through spectroscopic methods.

3.1.3. Binding forces and binding sites

Binding forces during AR-proteinase systems can be speculated from the variations of thermodynamic parameters including enthalpy change (ΔH), entropy change (ΔS), and free energy change (ΔG). The relationships among these thermodynamic parameters are expressed as: $\ln K_a = -\Delta H / RT + \Delta S/R$ and $\Delta G = \Delta H - T\Delta S$ (R and T are the gas constant and the temperature, respectively) [34]. Through the fluorescent data of AR-proteinase systems at three different temperatures, the linear fitting equations of AR-proteinase systems were $\ln K_a = 5861.38 / T - 8.87$ (J mol^{-1}) in AR-trypsin system and $\ln K_a = 7903.93 / T - 15.51$ (J mol^{-1}) in AR-pepsin system, respectively. The calculated ΔH, ΔS, and ΔG values were all negative (Table 1). Negative ΔG values suggested that the binding processes between AR and proteinases were occurred spontaneously [35]. Binding forces between compound and protein mainly include electrostatic interactions, hydrophobic bonds, hydrogen bonds, and van der Waals interactions [36]. Both negative ΔH and ΔS values in AR-proteinase systems indicated that hydrogen bonds and van der Waals interactions played vital roles among these binding interactions [35].

Detail binding forces and binding sites can be elucidated by molecular modeling [25]. Fig. 6A and B shows the lowest binding energy conformations of AR-trypsin system and AR-pepsin system. The docking

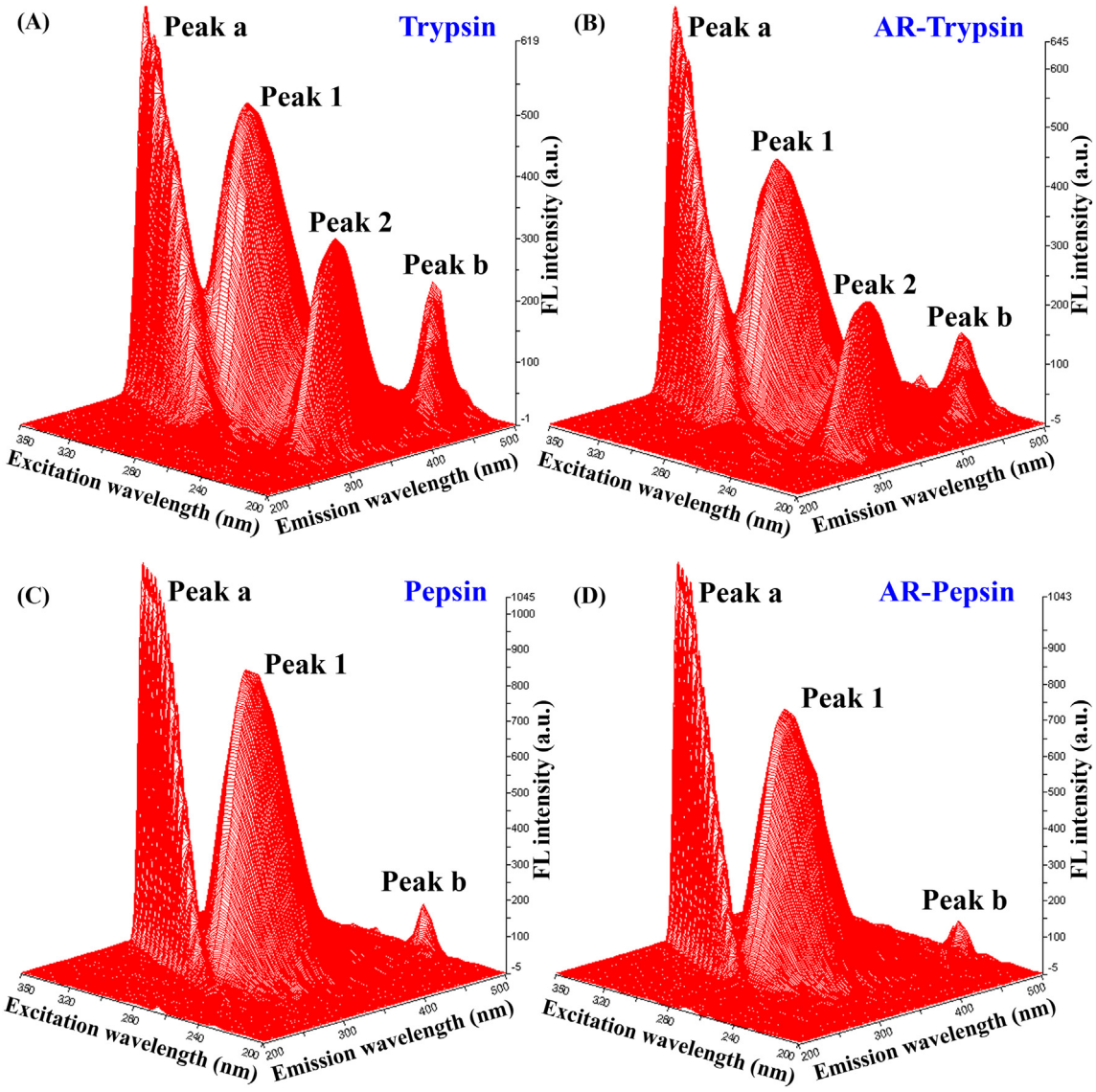

Fig. 8. Three-dimensional fluorescence spectra of trypsin (A), AR-trypsin system (B), pepsin (C), and AR-pepsin system (D). The concentrations of proteinases and AR were all 2.0×10^{-6} mol L^{-1}, respectively.

scores (stand for $-\log K_d$, and K_d is the dissociation constant) among AR-proteinase systems were 4.06 for AR-trypsin system and 5.96 for AR-pepsin system, suggesting that AR bound with proteinases from a very different binding direction. Since the higher docking score corresponded with the stronger binding ability between compound and the binding site [28], AR bound with pepsin more tightly than with trypsin. As further shown in Fig. 6C, eleven amino acid residues, including glutamine-50 (Gln-50), Trp-51, serine-86 (Ser-86), lysine-87 (Lys-87), Lys-107, leucine-108 (Leu-108), Lys-109, Ser-110, isoleucine-242 (Ile-242), alanine-243 (Ala-243), and asparagine-245 (Asn-245), took part in the binding interaction between AR and trypsin. As exhibited in Fig. 6D, twenty-one amino acid residues, containing aspartic acid-32 (Asp-32), glycine-34 (Gly-34), Ser-35, Ile-73, threonine-74 (Thr-74), Tyr-75, Gly-76, Thr-77, Ile-128, Tyr-189, Ile-213, Asp-215, Gly-217, Thr-218, Ser-219, Leu-220, Thr-222, glutamic acid-287 (Glu-287), methionine-289 (Met-289), proline-292 (Pro-292), and Ile-300, took part in the binding interaction between AR and pepsin. Obviously, the amino acid residues participated in the binding interaction of AR-pepsin system were more than those of AR-trypsin system, indicating the stronger binding ability of AR with pepsin. Ser, Tyr, Thr, and Lys amino acid resides are all polar amino acid residues, so van der Waals interactions should be involved in these binding interactions [37]. Furthermore, six hydrogen bonds were existed between the amino acid residues Gln-50 (2.06 Å), Trp-51 (2.74 Å), Lys-107 (2.10 and 2.28 Å), Lys-109 (1.93 Å), and Asn-245 (2.20 Å) of trypsin and AR molecule (Fig. 6E). Also, six hydrogen bonds were existed between the amino acid residues Thr-74 (1.99 Å), Gly-76 (2.28 Å), Tyr-189 (1.92 Å), Ser-219 (1.90 Å), Leu-220 (2.11 Å), and Glu-287 (2.10 Å) of pepsin and AR molecule (Fig. 6F). Thus, hydrogen bonds and van der Waals interactions played major roles in the binding interactions between AR and proteinases.

In addition, the distance between AR molecule and the nearest fluorescent amino acid Trp-51 of trypsin was calculated to be 2.63 Å (Fig. 7A), while the distances of two hydrogen bonds of AR with the fluorescent amino acid Tyr-75 and Tyr-189 of pepsin were 1.92 and 2.11 Å (Fig. 7B). Since the distances between AR and proteinases were very close, AR can quench the intrinsic fluorescence of proteinases dramatically. Moreover, the distances of AR molecule with the catalytic triad histidine-57 (His-57), aspartic acid-102 (Asp-102), and serine-195 (Ser-195) of trypsin [26] were 22.68, 20.67, and 21.61 Å, respectively (Fig. 7C). However, the distances of AR molecule with the catalytic twosome Asp-32 and Asp-215 of pepsin [27] were 4.81 and 3.89 Å,

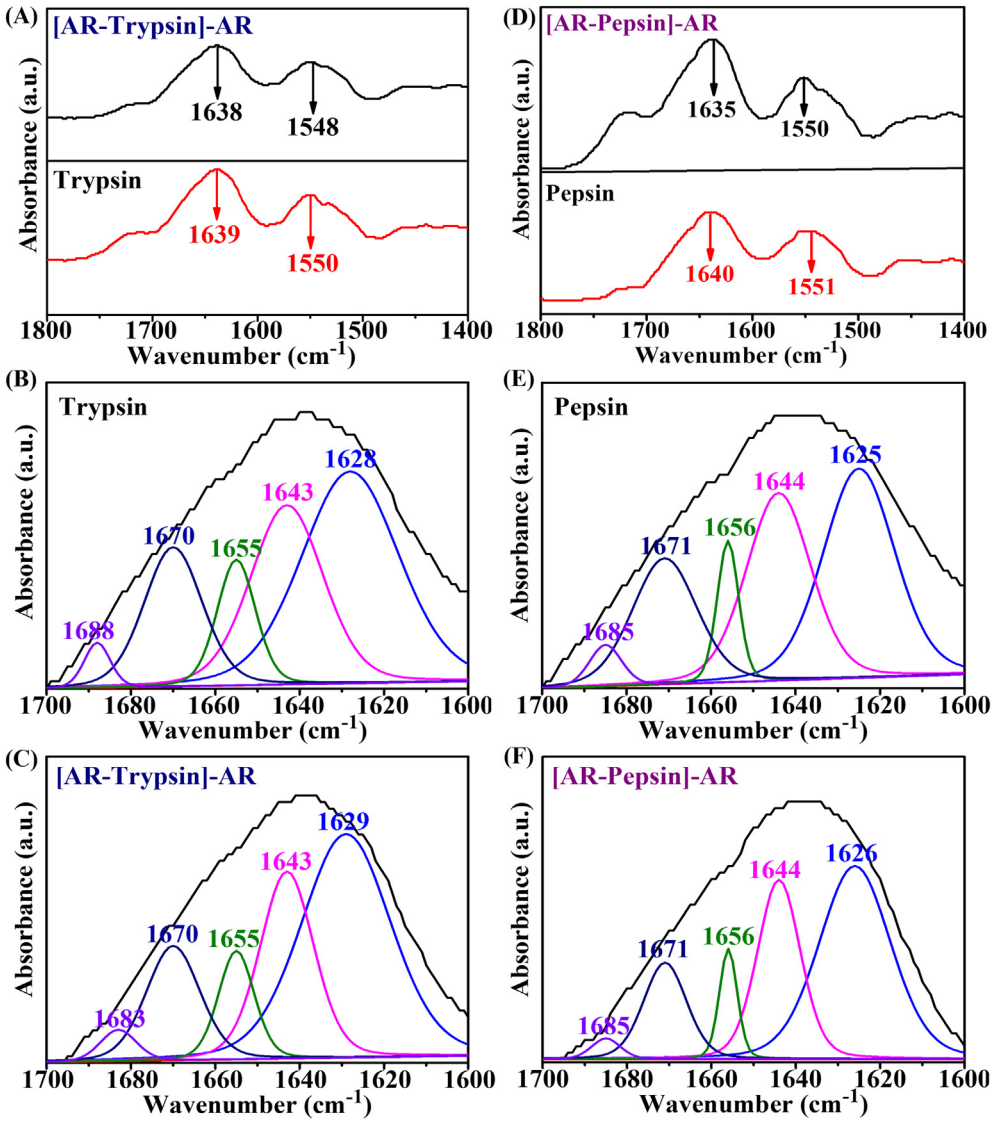

Fig. 9. FT-IR spectrum of trypsin and difference FT-IR spectrum between AR-trypsin system and AR (A), curve fitting of infrared amide I band in FT-IR spectrum of trypsin (B), and curve fitting of infrared amide I band in difference FT-IR spectrum between AR-trypsin system and AR (C). FT-IR spectrum of pepsin and difference FT-IR spectrum between AR-pepsin system and AR (D), curve fitting of infrared amide I band in FT-IR spectrum of pepsin (E), and curve fitting of infrared amide I band in difference FT-IR spectrum between AR-pepsin system and AR (F). The concentrations of proteinases and AR were all 1.0×10^{-3} mol L^{-1}.

respectively (Fig. 7D). Thus, AR did not bind directly with the enzymatic active-site residues of proteinases, and the enzymatic activity of pepsin should be affected by AR more obviously.

3.2. Conformational structures of proteinases affected by AR

3.2.1. Three-dimensional fluorescence spectrometry

Three-dimensional fluorescence spectrometry can be used to investigate the conformational structures of proteinases under the influence of AR. Fig. 8 presents the three-dimensional fluorescence spectra of proteinases and AR-proteinase systems. As shown in Fig. 8A, trypsin exhibited two fluorescent peaks (peak 1 and peak 2) and two scattering peaks (peak a and peak b). Fluorescent peak 1 ($\lambda_{ex/em}$ = 290/345 nm/nm) represented the fluorescent properties of amino acid residues and fluorescent peak 2 ($\lambda_{ex/em}$ = 235/342 nm/nm) meant the $\pi \rightarrow \pi^*$ transition in polypeptide backbone structure, respectively [38]. Scattering peak a and peak b indicated the Rayleigh ($\lambda_{em} = \lambda_{ex}$) and the second-order ($\lambda_{em} = 2\lambda_{ex}$) scattering peak, respectively [23]. After the addition of AR, both intensities of fluorescent peaks were all decreased from 512.9 to 440.5 for peak 1 and from 336.7 to 243.5 for peak 2, while the intensities of scattering peaks were changed from 619.9 to 645.1 for peak a and from 166.2 to 104.6 for peak b (Fig. 8B). These variations suggested the increment of the scattering effect and the significant change of conformational structure after the binding interaction of AR with trypsin. Same situations can be observed in the binding interaction between AR and pepsin except only one fluorescent peak 1 ($\lambda_{ex/em}$ = 290/348 nm/nm) in pepsin and AR-pepsin system [13]. After the addition of AR, the intensity of fluorescent peak 1 was decreased from 829.6 to 716.3 and the intensity of scattering peak b was decreased from 92.8 to 73.8 (Fig. 8C and D). These phenomena also proved the binding interaction of AR with pepsin and the conformational structure variation after such interaction.

3.2.2. FT-IR spectrometry

The secondary structures of proteins can be studied by FT-IR spectrometry, especially the curve fitting of the infrared amide I band of protein [12,24]. Usually, the infrared amide I band of protein is attributed as 1692 to 1680 cm^{-1} for β-antiparallel, 1680 to 1660 cm^{-1} for β-turn,

Table 3
Curve fitting data of infrared amide I bands of proteinases and AR-proteinases systems.

System	Peak (cm^{-1})	FWHM (cm^{-1})	Area	Relative percentage of area (%)
Trypsin	1628	27.4	0.433	43.3
	1643	20.6	0.274	27.4
	1655	10.7	0.101	10.1
	1670	16.5	0.168	16.8
	1688	7.8	0.024	2.4
AR-trypsin	1629	25.8	0.485	48.5
	1643	15.2	0.243	24.3
	1655	11.2	0.092	9.2
	1670	15.1	0.151	15.1
	1683	9.6	0.029	2.9
Pepsin	1625	21.4	0.379	37.9
	1644	19.3	0.305	30.5
	1656	8.4	0.075	7.5
	1671	18.5	0.207	20.7
	1685	9.7	0.034	3.4
AR-pepsin	1626	20.6	0.489	48.9
	1644	13.2	0.273	27.3
	1656	4.7	0.070	7.0
	1671	12.9	0.147	14.7
	1685	7.6	0.021	2.1

1660 to 1649 cm^{-1} for α-helix, 1648 to 1638 cm^{-1} for random coil, and 1637 to 1615 cm^{-1} for β-sheet structures, respectively [12,24]. As exhibited in Fig. 9A, trypsin exhibited an infrared amide I band at around 1639 cm^{-1} (C═O stretch), reflecting the secondary structures of trypsin [12]. Trypsin exhibited an infrared amide II band at about 1550 cm^{-1} (C—N stretch and N—H bending mode) reflecting the main peptide vibration bands in trypsin [12]. These bands of trypsin were changed to 1638 cm^{-1} for infrared amide I band and to 1548 cm^{-1} for infrared amide II band after binding with AR (black curve in Fig. 9A). So, AR interacted with trypsin, resulting in the rearrangement of the secondary structure in trypsin [24]. According to the curve fitting spectrum of infrared amide I band of trypsin (Fig. 9B), the peaks at 1688, 1670, 1655, 1643, and 1628 cm^{-1} were ascribed to the β-antiparallel, β-turn, α-helix, random coil, and β-sheet structures of trypsin, respectively. The relative percentages of various secondary structures were calculated and the results were exhibited in Table 3. The relative percentages of secondary structures of trypsin were 10.1% of α-helix, 43.3% of β-sheet (main secondary structure), 16.8% of β-turn, 2.4% of β-antiparallel, and 27.4% of random coil [12], respectively. At the present of AR, the peaks at 1683, 1670, 1655, 1643, and 1629 cm^{-1} were ascribed to the β-antiparallel, β-turn, α-helix, random coil, and β-sheet structures of trypsin, respectively (Fig. 9C). The relative percentages of secondary structures of trypsin were changed to 9.2% of α-helix, 48.5% of β-sheet, 15.1% of β-turn, 2.9% of β-antiparallel, and 24.3% of random coil, respectively. Therefore, the secondary structure of trypsin was changed from the mainly β-turn and random coil structures to the β-sheet structure.

On the other hand, the infrared amide I band and the infrared amide II band of pepsin were at around 1640 and 1551 cm^{-1}, respectively (Fig. 9D). These two bands of pepsin were changed to 1635 cm^{-1} for infrared amide I band and to 1550 cm^{-1} for infrared amide II band after binding with AR (black curve in Fig. 9D). As further shown in Fig. 9E, the peaks at 1685, 1671, 1656, 1644, and 1625 cm^{-1} reflected the β-antiparallel, β-turn, α-helix, random coil, and β-sheet structures of pepsin, respectively. As shown in Table 3, the relative percentages of secondary structures of pepsin were 7.5% of α-helix, 37.9% of β-sheet (main secondary structure), 20.7% of β-turn, 3.4% of β-antiparallel, and 30.5% of random coil [12], respectively. At the present of AR, the peaks at 1685, 1671, 1656, 1644, and 1626 cm^{-1} meant the β-antiparallel, β-turn, α-helix, random coil, and β-sheet structures of pepsin, respectively (Fig. 9F). The relative percentages of secondary

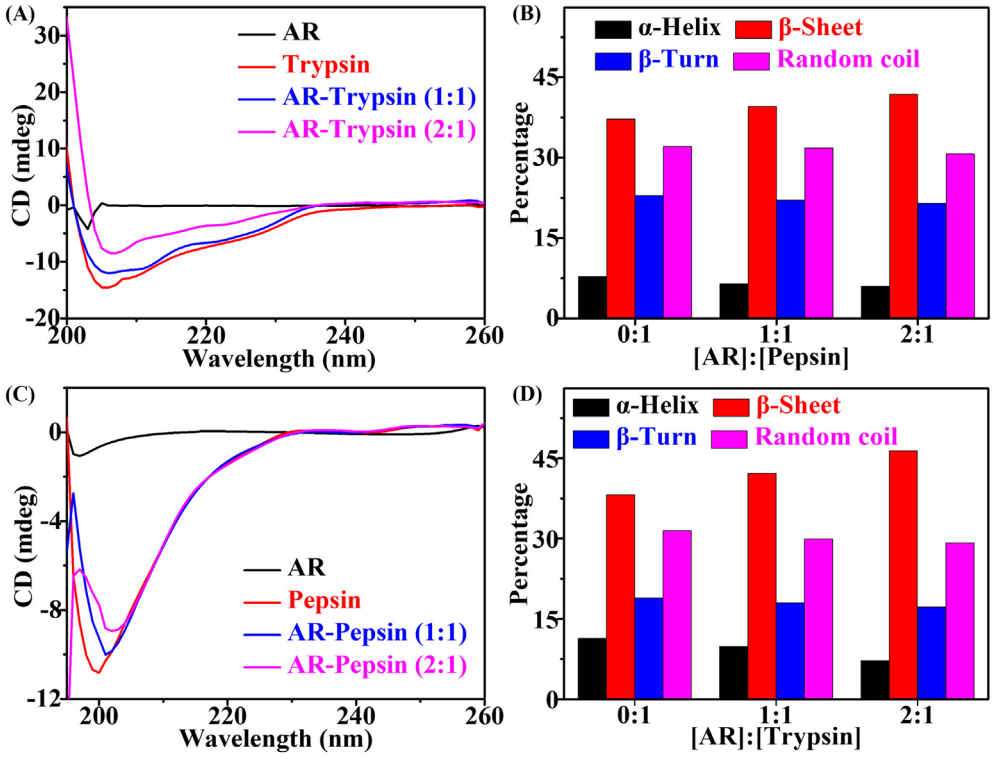

Fig. 10. (A) CD spectra of AR and trypsin in the presence of different concentrations of AR. (B) Percentages of different secondary structures of trypsin in the presence of different concentrations of AR. (C) CD spectra of AR and pepsin in the presence of different concentrations of AR. (D) Percentages of different secondary structures of pepsin in the presence of different concentrations of AR. The concentrations of trypsin and pepsin were 2.5×10^{-5} and 2.5×10^{-6} mol L^{-1}, while the concentrations of AR were one or two times higher than the concentrations of proteinases.

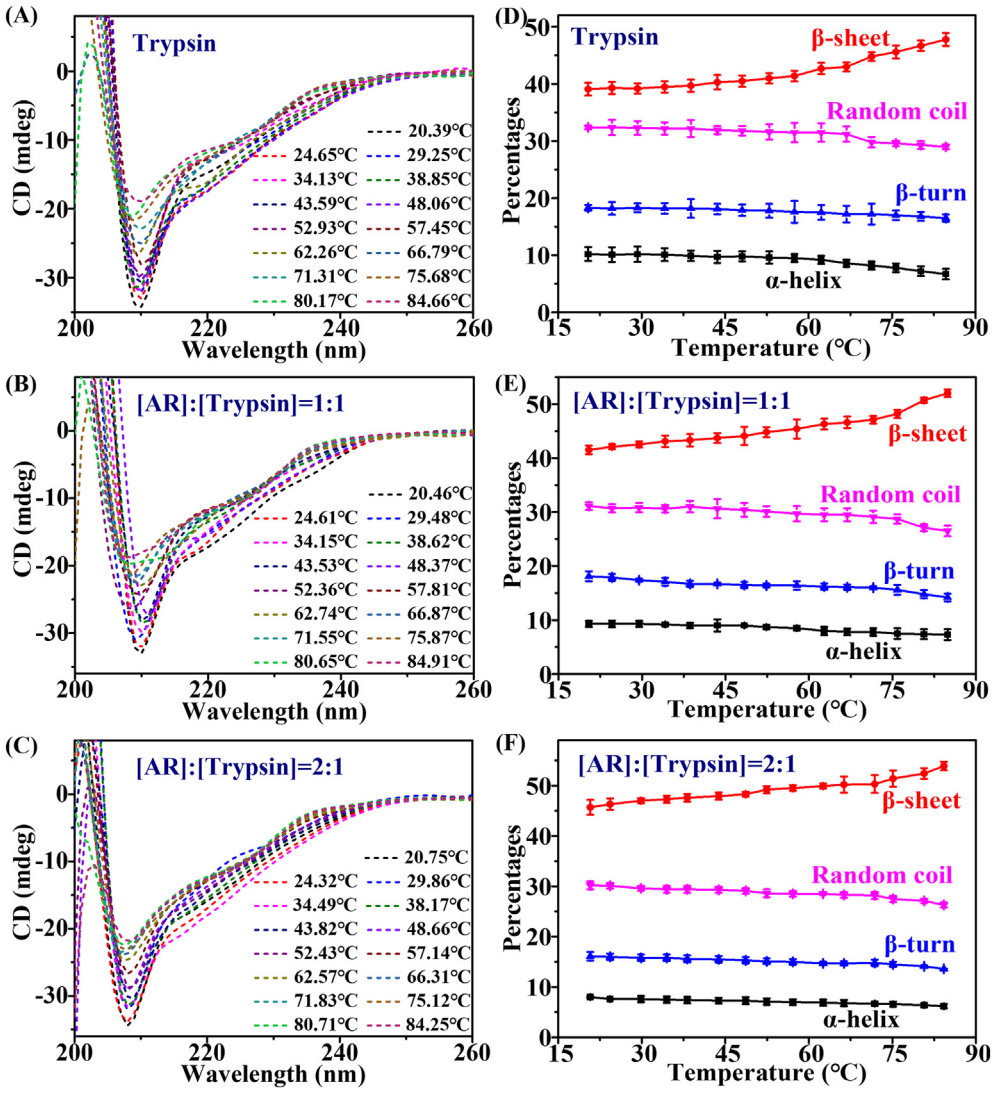

Fig. 11. (A to C) Temperature dependent CD spectra of trypsin and AR-trypsin system with different molar ratios. (D to F) Percentages of different secondary structures of trypsin in the presence of different concentrations of AR. The concentration of trypsin was 2.5×10^{-5} mol L^{-1}, while the concentration of AR was increased from 0 to 5.0×10^{-5} mol L^{-1} with interval of 2.5×10^{-5} mol L^{-1}.

structures of pepsin were 7.0% of α-helix, 48.9% of β-sheet, 14.7% of β-turn, 2.1% of β-antiparallel, and 27.3% of random coil in AR-pepsin system, respectively. Obviously, the secondary structure of pepsin was changed from the mainly β-turn and the random coil structures to the β-sheet structure. Such variations were highly consistent with those in AR-trypsin system. All these results implied that AR induced the secondary structure variations of both trypsin and pepsin, resulting in the enhanced hydrophobic environments and more stable conformations of proteinases. Comparably, after the addition of AR, the variation of the β-sheet structure in pepsin was much bigger than that in trypsin, suggesting that the conformational structure of pepsin was affected by AR more significantly and efficiently.

3.2.3. CD spectroscopy

The secondary structures of proteinases are continuously researched by CD spectroscopy [25,39]. Fig. 10A exhibited the CD spectra of AR and trypsin with different concentrations of AR. AR did not show any CD signal while trypsin showed a typical negative peak at around 206 nm [25], and AR caused a significant decrease of the absorbance of this band. According to the CDNN software [25], the percentages of secondary structures of trypsin were 11.4% of α-helix, 38.2% of β-sheet, 18.9% of β-turn, and 31.5% of random coil structures, respectively (Fig. 10B). When 2.5×10^{-5} mol L^{-1} of AR was present, the contents of α-helix and β-sheet structures were changed to 9.9% and 42.2%, respectively. When 5.0×10^{-5} mol L^{-1} of AR was present, the contents of α-helix and β-sheet structures were changed to 7.2% and 46.4%, respectively. Same changes were existed in AR-pepsin system with different concentrations of AR (Fig. 10C and D). Pepsin showed a characteristic negative peak at around 200 nm [14], and the absorbance of such peak was decreased gradually after the addition of increasing concentration of AR. The percentages of secondary structures of pepsin were calculated to be 7.8% of α-helix, 37.2% of β-sheet, 22.9% of β-turn, and 32.1% of random coil structures, respectively (Fig. 10D). When 2.5×10^{-6} mol L^{-1} of AR was present, the contents of α-helix and β-sheet structures were changed to 6.5% and 39.6%, respectively. When 5.0×10^{-6} mol L^{-1} of AR was present, the contents of α-helix and β-sheet structures were changed to 6.0% and 41.8%, respectively. These variations suggested that AR combined with the amino acid residues of proteinases and induced their partial structure folding [25], which agreed well with the results obtained by FT-IR spectrometry.

Besides those, to investigate the thermal stability of proteinases affected by AR, both T_m and ΔH_m values were measured by CD spectrometer equipped with the Global Analysis Software. Figs. 11 and 12 showed the temperature dependent CD spectra of AR-proteinase

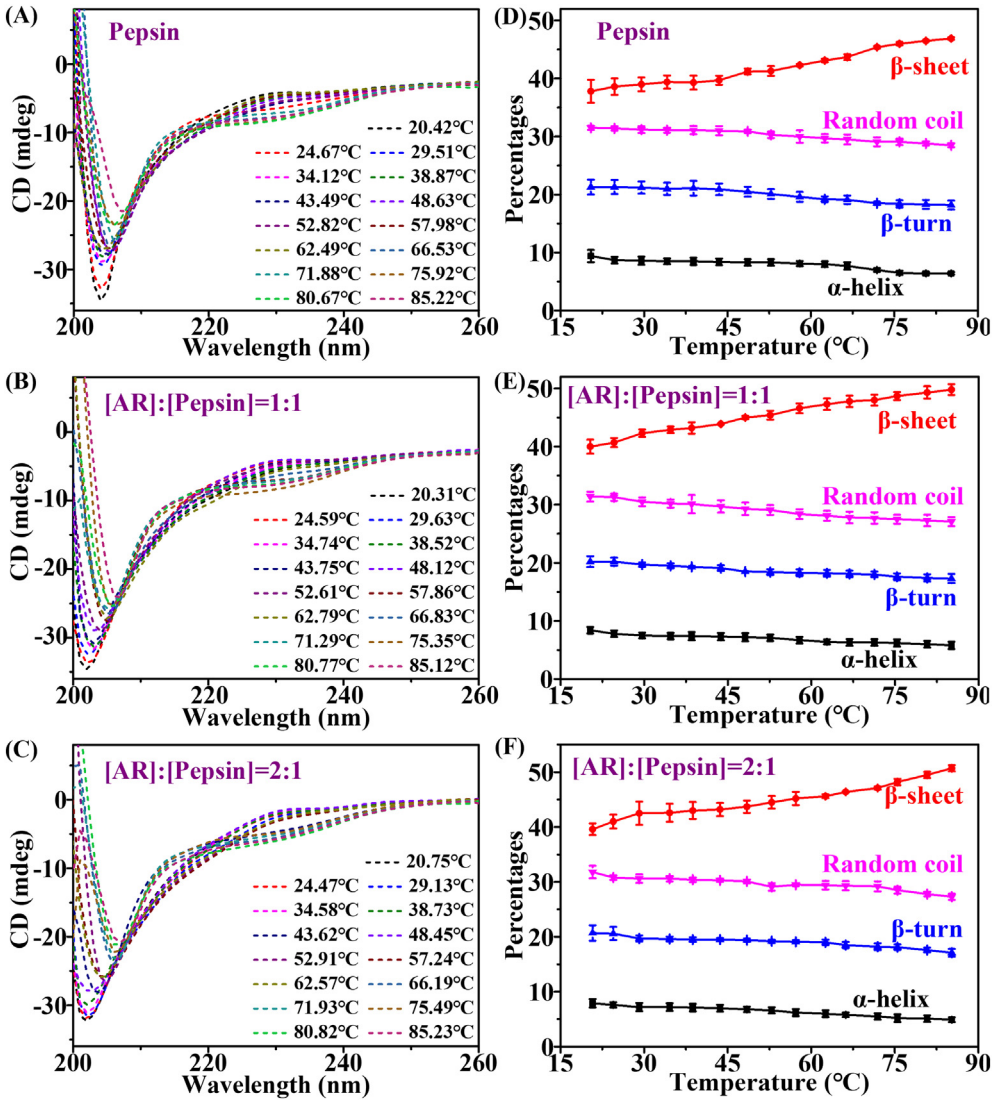

Fig. 12. (A to C) Temperature dependent CD spectra of pepsin and AR-pepsin system with different molar ratios. (D to F) Percentages of different secondary structures of pepsin in the presence of different concentrations of AR. The concentration of pepsin was 2.5×10^{-6} mol L^{-1}, while the concentration of AR was increased from 0 to 5.0×10^{-6} mol L^{-1} with interval of 2.5×10^{-6} mol L^{-1}.

systems with different molar ratios. Finally, the calculated T_m values of trypsin and pepsin were (66.8 ± 3.5) and (63.3 ± 0.8) °C, respectively. The T_m value of trypsin was decreased to (55.8 ± 1.7) and (49.9 ± 0.1) °C separately when the concentration of AR was one or two times higher than the concentration of trypsin. The T_m value of pepsin was also decreased to (57.3 ± 0.1) and (46.1 ± 0.1) °C separately when the concentration of AR was one or two times higher than the concentration of pepsin. Meanwhile, the ΔH_m value of trypsin was decreased from (254.7 ± 7.1) to (178.1 ± 7.4) and (100.5 ± 18) kJ mol^{-1} when the concentration of AR was increased to 2.5×10^{-5} and 5.0×10^{-5} mol L^{-1}, respectively. The ΔH_m value of pepsin was also decreased from (260.2 ± 0.92) to (210.7 ± 6.2) and (143.5 ± 30) kJ mol^{-1} when the concentration of AR was increased to 2.5×10^{-6} and 5.0×10^{-6} mol L^{-1}, respectively. Both the reductions of T_m and ΔH_m values confirmed that AR inhibited the thermal denaturation procedures of proteinases and reduced their thermal stabilities [25,39].

3.3. Activities of proteinases

3.3.1. Kinetic parameters of proteinases

Kinetic parameters of proteinases can be obtained through enzymatic reaction of trypsin on BApNA and pepsin on hemoglobin, since BApNA and hemoglobin were often degraded by trypsin and pepsin separately [20,21]. BApNA can be digested by trypsin to produce pNA, and the generation of pNA per minute (mol L^{-1} min^{-1}) is used to evaluate the trypsin activity [20]. Meanwhile, hemoglobin can be digested by pepsin to produce tyrosine, so the generation of tyrosine per minute (mol L^{-1} min^{-1}) is absolutely used to evaluate the pepsin activity [21]. The Michaelis-Menten curves from data of two enzymatic reactions with different concentrations of AR were shown in Fig. 13A and B. It is obvious that the enzyme reaction velocity (V) value was increased accordingly with the increase of the concentration of substate but this value was decreased dramatically with the addition of increasing concentration of AR under same substate concentration. Lineweaver-Burk plot was created by plotting the reciprocal of enzyme reaction velocity (V) against the reciprocal of the substrate concentration ([s]). Michael's constant (K_m) and the maximum reaction velocity (V_{max}) were obtained from the double-reciprocal plot [20,21]:

$$\frac{1}{V} = \frac{K_m}{V_{max}} \frac{1}{[s]} + \frac{1}{V_{max}} \tag{5}$$

The double-reciprocal plots of proteinases with various concentrations of substrates and AR were exhibited in Fig. 13C and D. As can be

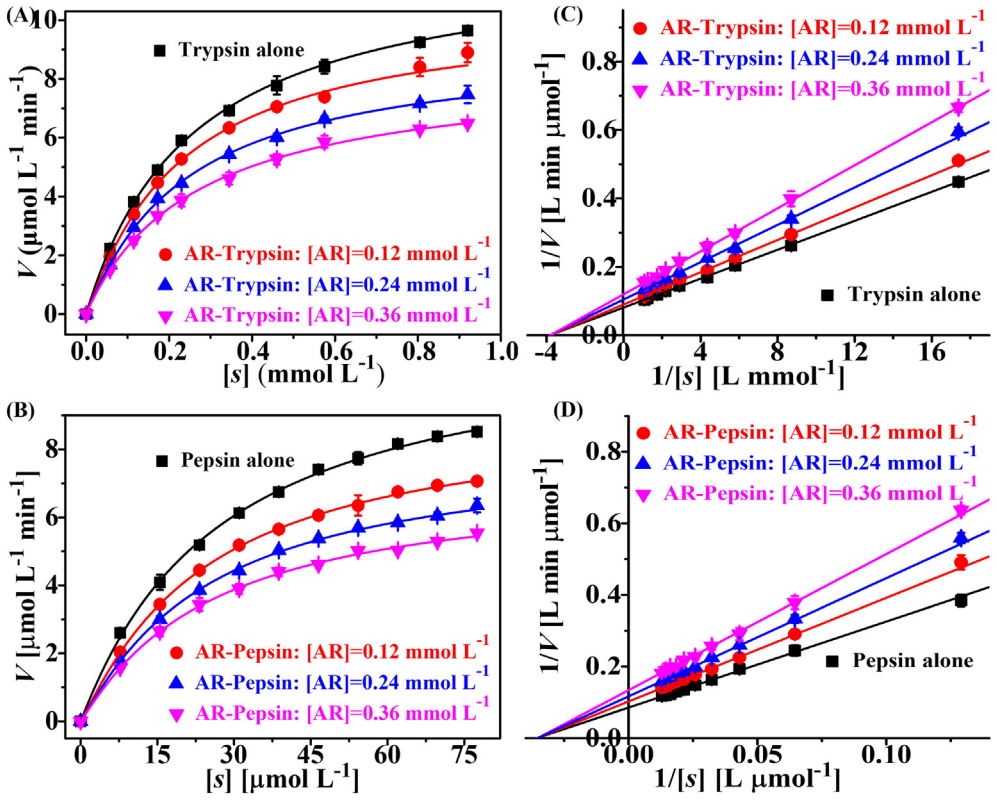

Fig. 13. (A) Michaelis-Menten curves from activity data of trypsin with different concentrations of AR. (B) Double-reciprocal plots of trypsin with different concentrations of AR. (C) Michaelis-Menten curves from activity data of pepsin with different concentrations of AR. (D) Double-reciprocal plots of pepsin with different concentrations of AR. The concentrations of trypsin and pepsin were 2.1×10^{-7} and 5.6×10^{-6} mol L^{-1}. The concentration of BApNA was increased from 5.7×10^{-5} to 9.2×10^{-4} mol L^{-1}. The concentration of hemoglobin was increased from 7.8×10^{-6} to 7.8×10^{-5} mol L^{-1}. The concentration of AR was increased from 0 to 3.6×10^{-4} mol L^{-1} with interval of 1.2×10^{-4} mol L^{-1}.

seen from Table 4, the K_m and V_{max} values of trypsin alone were $(2.60 \pm 0.01) \times 10^{-4}$ mol L^{-1} and $(1.23 \pm 0.02) \times 10^{-5}$ mol L^{-1} min^{-1}, respectively. Obviously, after the addition of AR, the V_{max} values was decreased dramatically but the K_m values was kept almost constant, reflecting the non-competitive inhibition mode of AR in the enzymatic activity of trypsin [40,41]. Meanwhile, the K_m and V_{max} values of pepsin alone were $(2.81 \pm 0.10) \times 10^{-5}$ mol L^{-1} and $(1.17 \pm 0.02) \times 10^{-5}$ mol L^{-1} min^{-1}, respectively. When AR was present, the K_m values remained almost constant and the V_{max} values was decreased gradually, also suggesting the non-competitive inhibition mode of AR in the enzymatic activity of pepsin [40]. Thus, AR could reduce the activities of trypsin and pepsin through non-competitive manner.

The catalytic constant (k_{cat}) of proteinase can be calculated through the equation of $k_{cat} = V_{max}$/[Proteinase], and the catalytic efficiency (k_{cat}/K_m) can be used to evaluate the enzymatic ability of proteinase [20]. Usually, the values of K_m, V_{max}, k_{cat}, and k_{cat}/K_m can efficiently evaluate the activity of proteinase, and the higher V_{max}, k_{cat}, and k_{cat}/K_m values but the lower K_m value suggest the stronger enzymatic activity of proteinase [20]. As shown in Table 4, both the k_{cat} and k_{cat}/K_m values in two enzymatic reactions were all decreased with the increasing concentration of AR, suggesting that AR inhibited the activities of proteinases through the concentration-dependent manner. When the concentration of AR was increased to 3.6×10^{-4} mol L^{-1}, both the k_{cat} and k_{cat}/K_m values of trypsin were reduced to 67.4% and 67.1% of their initial values. Comparably, the k_{cat} and k_{cat}/K_m values of pepsin were reduced to 64.1% and 63.4% of their initial values if 3.6×10^{-4} mol L^{-1} of AR was present. It is obvious that AR inhibited the activity of pepsin more efficiently, due to the longer distances between AR molecule and the catalytic triad His-57, Asp-102, and Ser-195 of trypsin.

3.3.2. SDS-PAGE

Trypsin and pepsin can digest numerous peptides, amidos, and ester bonds of Lys with arginine (Arg) and fluorescent amino acid residues in proteins, thus HSA was widely used as the substrate to evaluate the

Table 4
Kinetic parameters of two enzymatic reactions with different concentrations of AR (mean value ± standard deviation, $n = 3$).

AR (10^{-4} L mol^{-1})	Trypsin-BApNA				Pepsin-hemoglobin			
	K_m (10^{-4} mol L^{-1})	V_{max} (10^{-5} mol L^{-1} min^{-1})	k_{cat} (min^{-1})	k_{cat}/K_m (10^5 L mol^{-1} min^{-1})	K_m (10^{-5} mol L^{-1})	V_{max} (10^{-5} mol L^{-1} min^{-1})	k_{cat} (min^{-1})	k_{cat}/K_m (10^4 L mol^{-1} min^{-1})
0	2.60 ± 0.01	1.23 ± 0.02	58.6 ± 0.01	2.25 ± 0.07	2.81 ± 0.10	1.17 ± 0.02	2.09 ± 0.03	7.44 ± 0.28
1.2	2.61 ± 0.01	1.11 ± 0.10	52.9 ± 0.01	2.06 ± 0.06	2.82 ± 0.07	0.98 ± 0.06	1.75 ± 0.09	6.21 ± 0.11
2.4	2.61 ± 0.02	0.96 ± 0.01	45.7 ± 0.02	1.75 ± 0.11	2.83 ± 0.17	0.86 ± 0.04	1.54 ± 0.04	5.44 ± 0.09
3.6	2.62 ± 0.02	0.83 ± 0.01	39.5 ± 0.04	1.51 ± 0.01	2.84 ± 0.02	0.75 ± 0.01	1.34 ± 0.02	4.72 ± 0.02

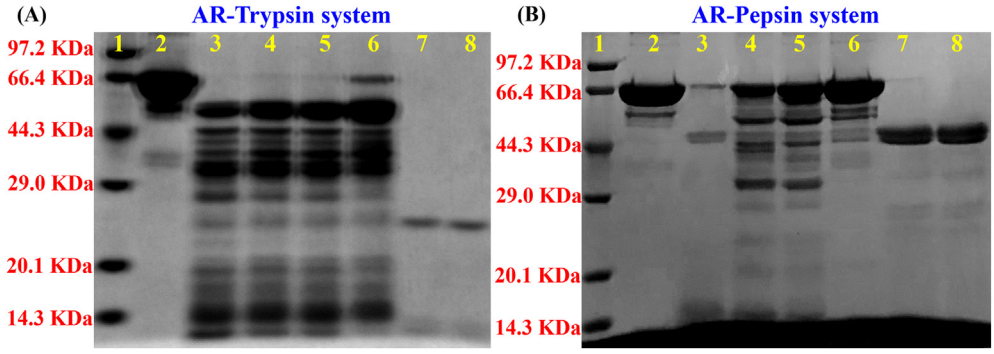

Fig. 14. (A) SDS-PAGE electropherogram demonstrating the low molecular weight marker (Line 1), HSA (Line 2), HSA-trypsin (Line 3), HSA-trypsin-AR (Lines 4 to 6), AR-trypsin (Line 7), and trypsin (Line 8), respectively. (B) SDS-PAGE electropherogram demonstrating the low molecular weight marker (Line 1), HSA (Line 2), HSA-pepsin (Line 3), HSA-pepsin-AR (Lines 4 to 6), AR-pepsin (Line 7), and pepsin (Line 8), respectively. The concentrations of HSA, trypsin, and pepsin were 6.0×10^{-6}, 2.5×10^{-5}, and 1.1×10^{-5} mol L^{-1}, respectively. The concentration of AR (from Lines 3 to 6) was increased from 0 to 2.4×10^{-2} mol L^{-1} with interval of 8.0×10^{-3} mol L^{-1}.

activity of proteinases via SDS-PAGE [42,43]. Fig. 14 shows SDS-PAGE electropherograms of HSA before or after the addition of proteinases and/or AR. Lines 1 in both Fig. 14A and B showed the migration band of the low molecular weight marker which was often used to estimate the molecular weights of the samples. This low molecular weight marker usually includes 97.2 KDa for phosphatase b, 66.4 KDa for bovine serum protein, 44.3 KDa for ovalbumin, 29.0 KDa for carbonic anhydrase, 20.1 KDa for trypsin inhibitor, and 14.3 KDa for lysozyme. HSA showed only one characteristic migration band with the molecular weight of around 66.4 KDa (lines 2 in both Fig. 14A and B). Trypsin and pepsin all exhibited only one characteristic migration band (lines 7 in both Fig. 14A and B), and 2.4×10^{-2} mol L^{-1} of AR did not affect the migration bands of proteinases at all (lines 8 in both Fig. 14A and B). After the enzymatic reactions by trypsin and pepsin, HSA was digested by proteinases to produce several small protein/peptide-rich product mixtures with the molecular weights of lower than 66.4 KDa, resulting in the existences of several migration bands with smaller molecular weights (lines 3 in both Fig. 14A and B). After the addition of 8.0×10^{-3} mol L^{-1} of AR, the colors of the migration bands with bigger molecular weights became dark but the colors of the migration bands with lower molecular weights became shallow (lines 4 in both Fig. 14A and B). When the concentration of AR was increased from 1.6×10^{-2} to 2.4×10^{-2} mol L^{-1}, the colors of the migration bands with bigger molecular weights became much obvious while the colors of the migration bands with lower molecular weights became much obscure (lines 5 to 6 in both Fig. 14A and B). All these phenomena confirmed the inhibition ability of AR on the digestion activities of proteinases for HSA. Most interestingly, the color of the migration band with molecular weight of around 66.4 KDa became clearer in AR-pepsin system, thus partial HSA was not digested by pepsin with the increasing concentration of AR from 8.0×10^{-3} to 2.4×10^{-2} mol L^{-1} (lines 4 to 6 in Fig. 14B). Therefore, AR could inhibit the activities of proteinases dramatically, but the inhibition ability of AR on pepsin activity was comparably stronger.

4. Conclusions

Herein, we comparably investigated the conformational structures and the activities of trypsin and pepsin after their binding interactions with AR. All results suggested that AR reacted with proteinases to form stable ground state complexes and statically quenched the intrinsic fluorescence of proteinases under the mainly binding forces of van der Waal interactions and hydrogen bonds. The conformational structures and the activities of proteinases were all affected by AR dramatically, resulting in the structure transformation to the β-sheet structure and the reduction of their enzymatic activities. Comparably, the binding interaction between AR and pepsin was relatively higher, causing the more significant variations in both conformational structure and enzymatic activity. These researches explored the potential toxicity of food colourant AR in biological fields.

Declaration of competing interest

The authors declare that they have no known competing financial interests or personal relationships that could have appeared to influence the work reported in this paper.

Acknowledgments

This work was financially supported by National Natural Science Foundation of China (21763005, 21864006), Natural Science Foundation of Guangxi Province (2017GXNSFDA198034, 2017GXNSFFA198005), Scientific Research and Technology Development Program of Guangxi (AD17195081), the Thousands of Young Teachers Training Program of Guangxi Province (guijiaoren[2018]18), the High-Level-Innovation Team (guijiaoren[2017]38) and Outstanding Scholar Project of Guangxi Higher Education Institutes, and BAGUI Scholar Program of Guangxi Province of China.

References

[1] N.A. Al-Shabib, J.M. Khan, A. Malik, P. Sen, S. Ramireddy, S. Chinnappan, S.F. Alamery, F.M. Husain, A. Ahmad, H. Choudhry, M.I. Khan, S.A. Shahzad, Allura red rapidly induces amyloid-like fibril formation in hen egg white lysozyme at physiological pH, Int. J. Biol. Macromol. 127 (2019) 297–305.
[2] G. Feketea, S. Tsabouri, Common food colorants and allergic reactions in children: myth or reality? Food Chem. 230 (2017) 578–588.
[3] K. Yamjala, M.S. Nainar, N.R. Ramisetti, Methods for the analysis of azo dyes employed in food industry - a review, Food Chem. 192 (2016) 813–824.
[4] Food and Drug Administration/Center for Food Safety and Applied Nutrition, Certified color additives in food and possible association with attention deficit hyperactivity disorder in children, http://www.fda.gov/AdvisoryCommittees/CommitteesMeetingMaterials/FoodAdvisoryCommittee/ucm149740.htm/ 2011 (Accessed 16.08.21).
[5] A. Basu, G.S. Kumar, Targeting proteins with toxic azo dyes: a microcalorimetric characterization of the interaction of the food colorant amaranth with serum proteins, J. Agric. Food Chem. 62 (2014) 7955–7962.
[6] L.H. Wang, G.W. Zhang, Y.P. Wang, Binding properties of food colorant allura red with human serum albumin in vitro, Mol. Biol. Rep. 41 (2014) 3381–3391.
[7] D. Wu, J. Yan, J. Wang, Q. Wang, H. Li, Characterisation of interaction between food colourant allura red AC and human serum albumin: multispectroscopic analyses and docking simulations, Food Chem. 170 (2015) 423–429.
[8] D. Masone, C. Chanforan, Study on the interaction of artificial and natural food colorants with human serum albumin: a computational point of view, Comput. Biol. Chem. 56 (2015) 152–158.
[9] C.A. Lelis, E.A. Hudson, G.M.D. Ferreira, G.M.D. Ferreira, L.H.M.D. Silva, M.D.C.H.D. Silva, M.S. Pinto, A.C.D.S. Pires, Binding thermodynamics of synthetic dye Allura Red with bovine serum albumin, Food Chem. 217 (2017) 52–58.

[10] K. Yao, P.L. Tan, Y.C. Luo, L.Z. Feng, L.G. Xu, Z. Liu, Y.Y. Li, R. Peng, Graphene oxide selectively enhances thermostability of trypsin, ACS Appl. Mater. Interfaces 7 (2015) 12270–12277.
[11] L. Momeni, B. Shareghi, A.A. Saboury, S. Farhadian, Comparative studies on the interaction of spermidine with bovine trypsin by multispectroscopic and docking methods, J. Phys. Chem. B 120 (2016) 9632–9641.
[12] Y.P. Wang, G.W. Zhang, L.H. Wang, Potential toxicity of phthalic acid esters plasticizer: interaction of dimethyl phthalate with trypsin in vitro, J. Agric. Food Chem. 63 (2015) 75–84.
[13] F.S. Mohseni-Shahri, F. Moeinpour, M. Nosrati, Spectroscopy and molecular dynamics simulation study on the interaction of sunset yellow food additive with pepsin, Int. J. Biol. Macromol. 115 (2018) 273–280.
[14] M. Ying, F.W. Huang, H.D. Ye, H. Xu, L.L. Shen, T.W. Huan, S.T. Huang, J.F. Xie, S.L. Tian, Z.L. Hu, Z.D. He, J. Lu, K. Zhou, Study on interaction between curcumin and pepsin by spectroscopic and docking methods, Int. J. Biol. Macromol. 79 (2015) 201–208.
[15] R. Gonçalves, N. Mateus, V.D. Freitas, Biological relevance of the interaction between procyanidins and trypsin: a multitechnique approach, J. Agric. Food Chem. 58 (2010) 11924–11931.
[16] Y.Q. Wang, C.Y. Tan, S.L. Zhuang, P.Z. Zhai, Y. Cui, Q.H. Zhou, H.M. Zhang, Z.H. Fei, In vitro and in silico investigations of the binding interactions between chlorophenols and trypsin, J. Hazard. Mater. 278 (2014) 55–65.
[17] L.L. Shen, H. Xu, F.W. Huang, Y. Li, H.F. Xiao, Z. Yang, Z.L. Hu, Z.D. He, Z.L. Zeng, Y.N. Li, Investigation on interaction between Ligupurpuroside A and pepsin by spectroscopic and docking methods, Spectrochim. Acta A 135 (2015) 256–263.
[18] X.L. Wu, W.P. Wang, T. Zhu, T. Liang, F.Q. Lu, W.Y. He, H.P. Zhang, Z.G. Liu, S.H. He, K.P. Gao, Z.D. He, Phenylpropanoid glycoside inhibition of pepsin, trypsin and α-chymotrypsin enzyme activity in Kudingcha leaves from *Ligustrum purpurascens*, Food Res. Int. 54 (2013) 1376–1382.
[19] W.Z. Shi, Y.Q. Wang, H.M. Zhang, Z.M. Liu, Z.H. Fei, Probing deep into the binding mechanisms of folic acid with α-amylase, pepsin and trypsin: an experimental and computational study, Food Chem. 226 (2017) 128–134.
[20] Y.C. Fan, X. Wang, J. Li, L.N. Zhang, L. Yang, P.F. Gao, Z.L. Zhou, Kinetic study of the inhibition of ionic liquids on the trypsin activity, J. Mol. Liq. 252 (2018) 392–398.
[21] Y.Y. Yue, Z.Y. Wang, Y.Y. Zhang, Z.X. Wang, Q.Z. Lv, J.M. Liu, Binding of triclosan and triclocarban to pepsin: DFT, spectroscopic and dynamic simulation studies, Chemosphere 214 (2019) 278–287.
[22] S. Huang, E.L. Yang, J.D. Yao, W. Su, Q. Xiao, Low-temperature rapid synthesis of nitrogen and phosphorus dual-doped carbon dots for multicolor cellular imaging and hemoglobin probing in human blood, Sens. Actuators B Chem. 265 (2018) 326–334.
[23] S. Huang, H.N. Qiu, S.Y. Lu, F.W. Zhu, Q. Xiao, Study on the molecular interaction of graphene quantum dots with human serum albumin: combined spectroscopic and electrochemical approaches, J. Hazard. Mater. 285 (2015) 18–26.
[24] G.W. Zhang, L. Wang, J.H. Pan, Probing the binding of the flavonoid diosmetin to human serum albumin by multispectroscopic techniques, J. Agric. Food Chem. 60 (2012) 2721–2729.
[25] Z.H. Zhu, Y.Q. Wang, Y.J. Kang, H.M. Zhang, Z.M. Zhang, Z.H. Fei, J. Cao, Graphene oxide destabilizes myoglobin and alters its conformation, Carbon 114 (2017) 449–456.
[26] Y.Y. Liu, G.W. Zhang, N. Zeng, S. Hu, Interaction between 8-methoxypsoralen and trypsin: monitoring by spectroscopic, chemometrics and molecular docking approaches, Spectrochim. Acta A 173 (2017) 188–195.
[27] Y.B. Shi, M. Liu, H. Yan, C. Cai, Q.Y. Guo, W.X. Pei, R.Y. Zhang, Z.P. Wang, J. Han, Mutual influence of piceatannol and bisphenol F on their interaction with pepsin: insights from spectroscopic, isothermal titration calorimetry and molecular modeling studies, Spectrochim. Acta A 206 (2019) 384–395.
[28] S. Huang, J.N. Xie, J.G. Cui, L. Liu, Y. Liang, Y. Liu, Q. Xiao, Comparative investigation of binding interactions between three steroidal compounds and human serum albumin: multispectroscopic and molecular modeling techniques, Steroids 128 (2017) 136–146.
[29] C.F. Niu, P.L. Yang, H.Y. Luo, H.Q. Huang, Y.R. Wang, B. Yao, Engineering of *yersinia phytases* to improve pepsin and trypsin resistance and thermostability and application potential in the food and feed industry, J. Agric. Food Chem. 65 (2017) 7337–7344.
[30] U. Kragh-Hansen, Molecular aspects of ligand binding to serum albumin, Pharmacol. Rev. 33 (1981) 17–53.
[31] J.R. Lakowicz, Principles of Fluorescence Spectroscopy, 3rd ed. Plenum Press, New York, 2006 277.
[32] C.B. Murphy, Y. Zhang, T. Troxler, V. Ferry, J.J. Martin, W.E. Jones, Probing Förster and Dexter energy-transfer mechanisms in fluorescent conjugated polymer chemosensors, J. Phys. Chem. B 108 (2004) 1537–1543.
[33] S. Huang, F.W. Zhu, Q. Xiao, Q. Zhou, W. Su, H.N. Qiu, B.Q. Hu, J.R. Sheng, C.S. Huang, Combined spectroscopy and cyclic voltammetry investigates the interaction between [(η^6-*p*-cymene)Ru(benzaldehyde-*N*(4)-phenylthiosemicarbazone)Cl]Cl anticancer drug and human serum albumin, RSC Adv. 4 (2014) 36286–36300.
[34] S. Huang, Y. Liang, J.G. Cui, J.N. Xie, Y. Liu, B.Q. Hu, Q. Xiao, Comparative investigation of binding interactions with three steroidal derivatives of $d(GGGT)_4$ G-quadruplex aptamer, Steroids 132 (2018) 46–55.
[35] D.P. Ross, S. Subramanian, Thermodynamics of protein association reactions: forces contributing to stability, Biochemistry 20 (1981) 3096–3102.
[36] D. Leckband, Measuring the forces that control protein interactions, Annu. Rev. Biophys. Biomol. Struct. 29 (2000) 1–26.
[37] Y.Q. Wang, Z.H. Zhu, H.M. Zhang, J. Chen, B.P. Tang, J. Cao, Investigation on the conformational structure of hemoglobin on graphene oxide, Mater. Chem. Phys. 182 (2016) 272–279.
[38] S.R. Feroz, S.B. Mohamad, N. Bujang, S.N.A. Malek, S. Tayyab, Multispectroscopic and molecular modeling approach to investigate the interaction of flavokawain B with human serum albumin, J. Agric. Food Chem. 60 (2012) 5899–5908.
[39] H.M. Zhang, Z.H. Zhu, Y.Q. Wang, Z.H. Fei, J. Cao, Changing the activities and structures of bovine serum albumin bound to graphene oxide, Appl. Surf. Sci. 427 (2018) 1019–1029.
[40] R. Sharma, Enzyme Inhibition: Mechanisms and Scope, InTech, 2012.
[41] B.G. Liu, H.Z. Xiao, J.Q. Li, S. Geng, H.J. Ma, G.Z. Liang, Interaction of phenolic acids with trypsin: experimental and molecular modeling studies, Food Chem. 228 (2017) 1–6.
[42] J. Carol-Visser, M.V.D. Schans, A. Fidder, A.G. Hulst, B.L.M.V. Baar, H. Irth, D. Noort, Development of an automated on-line pepsin digestion-liquid chromatography-tandem mass spectrometry configuration for the rapid analysis of protein adducts of chemical warfare agents, J. Chromatogr. B 870 (2008) 91–97.
[43] K. Langer, M.G. Anhorn, I. Steinhauser, S. Dreis, D. Celebi, N. Schrickel, S. Faust, V. Vogel, Human serum albumin (HSA) nanoparticles: reproducibility of preparation process and kinetics of enzymatic degradation, Int. J. Pharm. 347 (2008) 109–117.